Master QLMN
Experimental quantum computing

François-Marie Le Régent
francois-marie.le-regent@pasqal.com

Lecture 4 - Superconducting qubits

January 21$^{\text{st}}$ 2026

1 Objectives & Overview

These lecture notes provide an overview of superconducting circuits for quantum information processing, ranging from fundamental principles to advanced bosonic encoding schemes. Our goal is to understand how we can engineer artificial atoms using macroscopic electrical circuits. We will start by establishing a physical intuition linking mechanical systems to electrical ones, then move to the non-linear elements that allow us to define qubits in superconducting circuits, and finally explore how to protect quantum information using the infinite Hilbert space of harmonic oscillators. Here are the key themes that we will cover in this lecture:

- **Quantum Harmonic Oscillator (QHO):**
  - Establishing the correspondence between mechanical springs and LC circuits
  - Lagrangian and Hamiltonian formulation of circuit dynamics
  - Canonical quantization and phase space representations
- **The Transmon Qubit:**
  - Introducing the Josephson[1] Junction as a non-linear inductor to create anharmonicity.
  - Deriving the Transmon Hamiltonian and the Duffing oscillator model.
  - **Control & Readout:** Microwave drive, Rotating Wave Approximation (RWA), and dispersive readout.
  - **Coupling:** Capacitive coupling between qubits for 2-qubit gates.
- **Bosonic Encoding & Error Correction:**
  - Utilizing the infinite Hilbert space of harmonic oscillators for redundant encoding.
  - **Open Quantum Systems:** Modeling dissipation with the Lindblad master equation.
  - **Cat Codes:** Stabilizing coherent states $(|\alpha\rangle, |-\alpha\rangle)$ to suppress bit-flip noise.
  - **Bias-Preserving Gates:** Implementing operations that respect the noise bias structure.
  - **GKP Codes:** Translationally symmetric codes and symplectic geometry in phase space.

These notes were written for the **Experimental Quantum Computing and Error Correction** course of M2 Master QLMN, see the course's website for more information. They rely on the standard formalism of superconducting circuits typically found in [1] and for bosonic codes in [2]. Also, a really nice description of superconducting transmon qubits is accessible on the qiskit youtube channel, presented by Zlatko Minev.

> **Exercices for next week (2026-01-14)**
>
> 3, 4, 5, 7, 9, 11, 13, 16, 17, 18

2 Quantum Harmonic Oscillator

2.1 Classical Harmonic Oscillator

To understand superconducting qubits, it is helpful to start with a system you already know well: the mechanical harmonic oscillator. Recall from your earlier lectures that a simple spring or a mass on a spring is the foundational model for quantization.

---

[1] Nobel prize in 1973 for his theoretical predictions of the properties of a supercurrent through a tunnel barrier
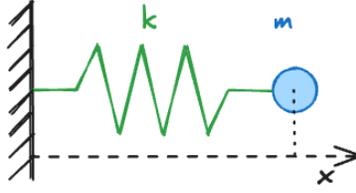
Figure 1: The classical spring as a 1D harmonic oscillator.

Recall: The Spring (1D Particle)

As shown in fig. 1, the Hamiltonian of a 1D particle is given by $\hat{H} = \frac{\hat{p}^2}{2m} + \frac{1}{2}k\hat{x}^2$, where $\hat{x}$ represents the position and $\hat{p}$ the momentum. The potential energy can be expressed using the frequency $\omega = \sqrt{k/m}$ as $\frac{1}{2}m\omega^2\hat{x}^2$. In the quantum regime, we introduced **Ladder Operators:**

- **Annihilation operator ($\hat{a}$):** $\hat{a} = \sqrt{\frac{m\omega}{2\hbar}}\left(\hat{x} + \frac{i}{m\omega}\hat{p}\right)$.
- **Creation operator ($\hat{a}^\dagger$):** $\hat{a}^\dagger = \sqrt{\frac{m\omega}{2\hbar}}\left(\hat{x} - \frac{i}{m\omega}\hat{p}\right)$.
- **Position and Momentum relations:** $\hat{x} \propto (\hat{a}^\dagger + \hat{a})$ and $\hat{p} \propto (\hat{a}^\dagger - \hat{a})$.

Action on Fock States $|n\rangle$:

- $\hat{a}|n\rangle = \sqrt{n}|n-1\rangle$.
- $\hat{a}^\dagger|n\rangle = \sqrt{n+1}|n+1\rangle$.
- **Commutator:** $[\hat{a}, \hat{a}^\dagger] = 1$.

These operators allow us to write the Hamiltonian in its quantized form, $\hat{H} = \hbar\omega\left(\hat{n} + \frac{1}{2}\right)$, where the number operator $\hat{n} = \hat{a}^\dagger\hat{a}$ counts the number of excitations in the system.

Exercise 1: Hamiltonian in Ladder Operators

Substitute $\hat{x}$ and $\hat{p}$ with $\hat{a}$ and $\hat{a}^\dagger$ in the harmonic oscillator Hamiltonian to derive $\hat{H} = \hbar\omega(\hat{n} + 1/2)$.

Answer

Pretty straightforward but important to do it at least once: From $\hat{x} = \sqrt{\frac{\hbar}{2m\omega}}(\hat{a}^\dagger + \hat{a})$ and $\hat{p} = i\sqrt{\frac{m\omega\hbar}{2}}(\hat{a}^\dagger - \hat{a})$:

$$\hat{H} = \frac{\hat{p}^2}{2m} + \frac{1}{2}m\omega^2\hat{x}^2 = \frac{\hbar\omega}{4}\left[-(\hat{a}^\dagger - \hat{a})^2 + (\hat{a}^\dagger + \hat{a})^2\right]$$

Expanding: $(\hat{a}^\dagger + \hat{a})^2 = \hat{a}^{\dagger 2} + \hat{a}^\dagger\hat{a} + \hat{a}\hat{a}^\dagger + \hat{a}^2$ and $(\hat{a}^\dagger - \hat{a})^2 = \hat{a}^{\dagger 2} - \hat{a}^\dagger\hat{a} - \hat{a}\hat{a}^\dagger + \hat{a}^2$

$$\hat{H} = \frac{\hbar\omega}{4}(2\hat{a}^\dagger\hat{a} + 2\hat{a}\hat{a}^\dagger) = \frac{\hbar\omega}{2}(\hat{a}^\dagger\hat{a} + \hat{a}\hat{a}^\dagger)$$

Using $[\hat{a}, \hat{a}^\dagger] = 1 \Rightarrow \hat{a}\hat{a}^\dagger = \hat{a}^\dagger\hat{a} + 1$:

$$\hat{H} = \hbar\omega\left(\hat{a}^\dagger\hat{a} + \frac{1}{2}\right) = \hbar\omega\left(\hat{n} + \frac{1}{2}\right)$$

Exercise 2: Commutator of Ladder Operators

Show that $[\hat{a}, \hat{a}^\dagger] = 1$ using the definitions of $\hat{a}$ and $\hat{a}^\dagger$ and the canonical commutation relation $[\hat{x}, \hat{p}] = i\hbar$.

Answer

Nothing complicated here: With $\hat{a} = \sqrt{\frac{m\omega}{2\hbar}}(\hat{x} + \frac{i}{m\omega}\hat{p})$ and $\hat{a}^\dagger = \sqrt{\frac{m\omega}{2\hbar}}(\hat{x} - \frac{i}{m\omega}\hat{p})$:

$$[\hat{a}, \hat{a}^\dagger] = \frac{m\omega}{2\hbar}\left[\hat{x} + \frac{i}{m\omega}\hat{p}, \hat{x} - \frac{i}{m\omega}\hat{p}\right]$$

$$= \frac{m\omega}{2\hbar}\left(-\frac{i}{m\omega}[\hat{x}, \hat{p}] + \frac{i}{m\omega}[\hat{p}, \hat{x}]\right) = \frac{m\omega}{2\hbar} \cdot \frac{-2i}{m\omega}[\hat{x}, \hat{p}]$$

$$= \frac{-i}{\hbar}[\hat{x}, \hat{p}] = \frac{-i}{\hbar}(i\hbar) = 1$$

Now, let's translate this mechanical intuition into electrical circuit variables. In an classical LC circuit, we don't have a mass or a spring, but we have **charge** and **flux** which behave as conjugate variables.

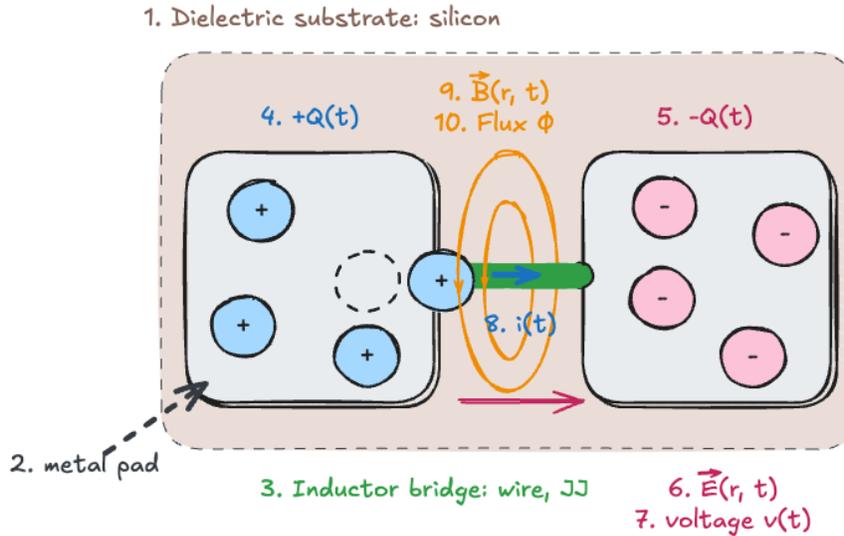### 2.1.1 Electrical Variables and Physical Intuition

Figure 2: Schematic of a classical electric circuit model featuring two metal islands (grey) connected by an inductive element (green) on a silicon substrate (light brown) (1) **Dielectric substrate:** silicon (2) **Metal pad** (3) **Inductor bridge:** wire, Josephson Junction (4) **+Q(t)** Positive charge on the left island (5) **-Q(t)** Negative charge on the right island (6) $\vec{E}(r,t)$ Electric field vector between the pads (7) **Voltage** $v(t)$ (8) $i(t)$ Current flowing through the bridge (9) $\vec{B}(r,t)$ Magnetic field vector around the current (10) **Flux** Φ Magnetic flux generated by the current

In electrical circuits, see fig. 2, the charge (Q) is defined as the integral of current over time, $Q = \int i\, dt$, and moving charges correspond to current. For a capacitor, the relationship is given by $Q = CV$. Flux (Φ) is defined as the integral of voltage over time, $\Phi = \int V\, dt$, and the motion of charges generates a magnetic field $(\vec{B})$ and associated flux. In the case of an inductor, the flux is $\Phi = Li$. The total energy $(\mathcal{E})$ in the circuit is

obtained by integrating the power, $P(t) = V(t) \cdot i(t)$, over time, giving $\mathcal{E}(t) = \int P(\tau) \, d\tau$. Specifically, the energy stored in the capacitor is $E_{cap} = \frac{1}{2}C\dot{\Phi}^2$, while the energy stored in the inductor is $E_{ind} = \frac{\Phi^2}{2L}$.

> **Intuition: The LC Circuit as a Spring**
>
> We can map the LC circuit to a spring in two ways:
>   1. **Charge as Position (The "Classical" View)**:
>   - Charge $Q \leftrightarrow$ Position x
>   - Inductor $L \leftrightarrow$ Mass m (Inertia against current change $\ddot{Q}$)
>   - Capacitor $1/C \leftrightarrow$ Spring constant k (Restoring force from accumulated charge)
>   - This is intuitive for classical circuits but problematic for quantum circuits with Josephson Junctions.
>   2. **Flux as Position (The "Quantum" View - Used Here)**:
>   - Flux $\Phi \leftrightarrow$ Position x
>   - Capacitor $C \leftrightarrow$ Mass m (Kinetic energy term $\frac{1}{2}C\dot{\Phi}^2 \sim \frac{1}{2}mv^2$)
>   - Inductor $1/L \leftrightarrow$ Spring constant k (Potential energy term $\frac{\Phi^2}{2L} \sim \frac{1}{2}kx^2$)
>
> **Why do we use the second one?** The Josephson Junction acts like a non-linear inductor. Its energy $U(\Phi) \propto -\cos(\Phi)$ depends on flux. If we treat flux as "position," this just becomes a non-linear potential energy (like a non-linear spring), which is easy to handle in the Hamiltonian. If we treated flux as "momentum," we'd have a "cosine kinetic energy," which is a mathematical nightmare!
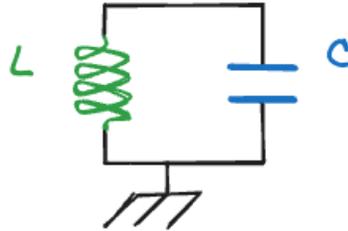
2.1.2 Kirchhoff's Network Laws

Figure 3: LC Circuit.

Using the nodes and loops of the circuit we can derive the equation of motion. **Kirchhoff's Current Law (KCL)** states that $\sum_{b \in \text{node}} \pm \dot{Q}_b(t) = 0$ (conservation of charge). At a node n_1 between the capacitor and the inductor, this implies $\dot{Q}_C + \dot{Q}_L = 0$. Similarly, **Faraday's Law of Induction** (or Kirchhoff's Voltage Law) requires $\sum_{b \in \text{node}} \pm \dot{\Phi}_b(t) = 0$. At node n_1, this gives $\dot{\Phi}_C - \dot{\Phi}_L = 0$, implying $\Phi_C = \Phi_L$.

Given $Q = CV \implies \dot{Q} = C\dot{V} = C\ddot{\Phi}$, and $i = \Phi/L$, we obtain the second-order differential equation for harmonic motion:

$$C\ddot{\Phi} + \frac{\Phi}{L} = 0$$

> **Exercise 3: LC Equation of Motion**
>
> Derive the equation of motion $C\ddot{\Phi} + \Phi/L = 0$ starting from Kirchhoff's laws applied to the LC circuit.

Again pretty straightforward. **KCL at node:** $i_C + i_L = 0$ (currents sum to zero) **For capacitor:** $i_C = C\frac{dV}{dt} = C\ddot{\Phi}$ (since $V = \dot{\Phi}$) **For inductor:** $i_L = \frac{\Phi}{L}$ (from $\Phi = Li_L$) Substituting into KCL:

$$C\ddot{\Phi} + \frac{\Phi}{L} = 0$$

This is a harmonic oscillator equation with $\omega_0 = 1/\sqrt{LC}$.

The solution describes a harmonic oscillation:

$$\ddot{\Phi} = -\omega_0^2 \Phi, \quad \text{where } \omega_0 = \frac{1}{\sqrt{LC}}$$

$$\Phi(t) = \Phi_0 e^{-i\omega_0 t}$$

Note:

In this flux-based representation, it is the magnetic flux Φ that oscillates. Notice there is no explicit Q in the final equation of motion, just as p doesn't appear in the Newton's law form $m\ddot{x} + kx = 0$.

2.2 The Hamiltonian for the Harmonic Oscillator

Rather than deriving the system from the Lagrangian and performing a Legendre transformation, we can obtain the Hamiltonian more directly by summing the energies stored in the elements of the circuit.

The Hamiltonian $\mathcal{H}$ for an LC circuit is defined in terms of the conjugate variables, with the flux Φ playing the role of generalized position and the charge Q as generalized momentum. The total energy is given by the sum of the electrostatic energy in the capacitor and the magnetic energy in the inductor:

$$\mathcal{H}(\Phi, Q) = \mathcal{E}_{\text{kinetic}} + \mathcal{E}_{\text{potential}} = \frac{Q^2}{2C} + \frac{\Phi^2}{2L}$$

In this expression, the term $\frac{Q^2}{2C}$ represents the electrostatic energy, which acts as the analog of kinetic energy $p^2/2m$ in mechanics. Meanwhile, $\frac{\Phi^2}{2L}$ corresponds to the magnetic energy stored in the inductor, analogous to the mechanical potential energy $\frac{1}{2}kx^2$.

Intuition: Why Flux and Charge?

Why are flux (Φ) and charge (Q) conjugate variables like position and momentum?
In quantum mechanics, you cannot know position and momentum simultaneously with infinite precision. Similarly, in a quantum circuit, you cannot know the exact number of Cooper pairs on the capacitor island (Q) and the exact generalized flux (Φ, which is proportional to the superconducting phase ϕ) at the same time. This uncertainty relation $[\hat{\Phi}, \hat{Q}] = i\hbar$ is central to understanding why quantum circuits behave differently from classical ones.

To verify that Φ and Q are indeed canonically conjugate variables, we turn to Hamilton's equations of motion. This approach allows us to recover the fundamental relations for voltage and current in the circuit. First, consider the equation for velocity. The time evolution of the "position" coordinate, Φ, is given by $\dot{\Phi} = \frac{\partial \mathcal{H}}{\partial Q}$. Taking the derivative of the Hamiltonian with respect to Q, we find $\frac{\partial \mathcal{H}}{\partial Q} = \frac{Q}{C}$. Since $Q = CV$, where V is the

voltage across the capacitor, this gives $\dot{\Phi} = V$. This equation matches the definition of magnetic flux, as voltage is the time derivative of flux according to Faraday's law. Next, consider the equation associated with force. The time evolution of the "momentum" coordinate Q is given by $\dot{Q} = -\frac{\partial \mathcal{H}}{\partial \Phi}$. When we differentiate the Hamiltonian with respect to Φ, we get $-\frac{\partial \mathcal{H}}{\partial \Phi} = -\frac{\Phi}{L}$. Recall that the flux in an inductor is given by $\Phi = L \cdot I_L$, where I_L is the current through the inductor, which leads to $\dot{Q} = -I_L$. Because $\dot{Q}$ represents the current flowing into the capacitor (denoted I_C), this equation can be rewritten as $I_C = -I_L$, or $I_C + I_L = 0$. This result directly reflects Kirchhoff's current law for a closed LC circuit.

Exercise 4: Equation of Motion

Combine the two results derived above ($\dot{\Phi} = Q/C$ and $\dot{Q} = -\Phi/L$) to find a second-order differential equation for Φ. Verify that this matches the standard harmonic oscillator equation $\ddot{\Phi} + \omega_0^2 \Phi = 0$, where $\omega_0 = 1/\sqrt{LC}$.

Answer

Simple substitution of variables. From $\dot{\Phi} = Q/C$, we get $Q = C\dot{\Phi}$. Taking the time derivative: $\dot{Q} = C\ddot{\Phi}$. Substituting into $\dot{Q} = -\Phi/L$:

$$C\ddot{\Phi} = -\frac{\Phi}{L} \quad \Rightarrow \quad \ddot{\Phi} = -\frac{1}{LC}\Phi$$

This gives: $\ddot{\Phi} + \omega_0^2 \Phi = 0$ with $\omega_0 = \frac{1}{\sqrt{LC}}$

Exercise 5: Hamiltonian from Lagrangian

Starting from the Lagrangian $\mathcal{L} = \mathcal{E}_{kin} - \mathcal{E}_{pot} = \frac{1}{2}C\dot{\Phi}^2 - \frac{\Phi^2}{2L}$, calculate the conjugate momentum $Q = \frac{\partial \mathcal{L}}{\partial \dot{\Phi}}$ and perform the Legendre transformation $\mathcal{H} = \dot{\Phi}Q - \mathcal{L}$ to verify the expression for the Hamiltonian given in the text.

Answer

The Lagrangian may be out of the scope of the lecture but if you are interested: **Conjugate momentum:**

$$Q = \frac{\partial \mathcal{L}}{\partial \dot{\Phi}} = \frac{\partial}{\partial \dot{\Phi}}\left(\frac{1}{2}C\dot{\Phi}^2\right) = C\dot{\Phi}$$

Hence $\dot{\Phi} = Q/C$. **Legendre transformation:**

$$\mathcal{H} = \dot{\Phi}Q - \mathcal{L} = \frac{Q}{C} \cdot Q - \left(\frac{1}{2}C\dot{\Phi}^2 - \frac{\Phi^2}{2L}\right)$$

$$= \frac{Q^2}{C} - \frac{1}{2}C\left(\frac{Q}{C}\right)^2 + \frac{\Phi^2}{2L} = \frac{Q^2}{C} - \frac{Q^2}{2C} + \frac{\Phi^2}{2L}$$

$$\mathcal{H} = \frac{Q^2}{2C} + \frac{\Phi^2}{2L}$$

> **Intuition**
>
> Another way to represent this is that the electric charges on the capacitor are flowing through the inductor to the other plate and back and forth: $\oplus Q \implies \text{flux} \implies \ominus Q$ (aka flip polarity of capacitor).
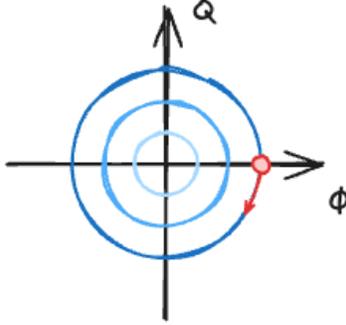

Figure 4: Classical phase space.

Using phase space representation, we can express the circular motion using $\mathbb{C}$ numbers:

$$\alpha(t) = \sqrt{\frac{1}{2\hbar Z}}(\Phi(t) + iZQ(t))$$

α is the classical analog to the bosonic ladder operator. The Hamiltonian can be rewritten using α as:

$$\mathcal{H} = \frac{Q^2}{2C} + \frac{\Phi^2}{2L} = \frac{1}{2}\hbar\omega_0(\alpha^*\alpha + \alpha\alpha^*)$$

2.3 Canonical Quantization

Transitioning from classical to quantum mechanics involves promoting our variables to operators, a process known as **Dirac's**[2] **Canonical Quantization** [3].

> **Full Canonical Quantization**
>
> Dirac's Canonical Quantization also involves replacing the Poisson bracket with the commutator, which we are not going to discuss in this lecture. For reference, here is the correspondence:
>
> | Classical (Poisson bracket) | Quantum (commutator) |
> | --- | --- |
> | $\{x, p\}_P = 1$ | $-\frac{i}{\hbar}[\hat{x}, \hat{p}] = \hat{1}$ |
> | $\frac{d}{dt}\mathcal{O} = \{\mathcal{O}, \mathcal{H}\}_P$ | $\frac{d}{dt}\hat{\mathcal{O}} = -\frac{i}{\hbar}[\hat{\mathcal{O}}, \hat{H}]$ |
>
> Where the Poisson bracket and commutator definitions are:
> - **Poisson Bracket:** $\{A, B\}_P = \frac{\partial A}{\partial \Phi}\frac{\partial B}{\partial Q} - \frac{\partial B}{\partial \Phi}\frac{\partial A}{\partial Q}$
> - **Commutator:** $[A, B] = AB - BA$

---

[2]Nobel prize in 1933 for the discovery of new productive forms of atomic theory

Exercise 6: Flux-Charge Commutator

Using the canonical quantization rule $[\hat{x}, \hat{p}] = i\hbar$, identify the correspondence $\hat{x} \to \hat{\Phi}$ and $\hat{p} \to \hat{Q}$ to show that $[\hat{\Phi}, \hat{Q}] = i\hbar$.

Answer

This one was pretty obvious from the correspondence table above: Position $\hat{x} \leftrightarrow$ Flux $\hat{\Phi}$ and Momentum $\hat{p} \leftrightarrow$ Charge $\hat{Q}$. By canonical quantization, conjugate variables satisfy the fundamental commutation relation. Since (Φ, Q) are the conjugate pair (verified via Hamilton's equations), we directly obtain:

$$[\hat{\Phi}, \hat{Q}] = i\hbar$$

This is the circuit analog of $[\hat{x}, \hat{p}] = i\hbar$.

2.3.1 Classical & Quantum Oscillator Comparison

The following table provides a side-by-side comparison between the classical and quantum descriptions of the harmonic oscillator, as applied to LC circuits. It highlights the correspondence between classical concepts (like phase space and Poisson brackets) and their quantum analogs (such as ladder operators and commutators).

	Classical	Quantum
Hamiltonian	$\mathcal{H} = \dfrac{Q^2}{2C} + \dfrac{\Phi^2}{2L} = \dfrac{1}{2}\hbar\omega_0(\alpha^*\alpha + \alpha\alpha^*)$	$\hat{H} = \dfrac{\hat{\Phi}^2}{2L} + \dfrac{\hat{Q}^2}{2C} = \hbar\omega_0(\hat{a}^\dagger\hat{a} + \hat{a}\hat{a}^\dagger)$
Phase Space	Points in phase space (Φ, Q) form circles; can use a single complex number $\alpha \in \mathbb{C}$ to describe motion.	Quantum states live in Hilbert space; evolution described by operators $(\hat{a}, \hat{a}^\dagger)$
Complex Amplitude (α)	$\alpha(t) = \sqrt{\dfrac{1}{2\hbar Z}}(\Phi(t) + iZQ(t))$Time evolution: $\alpha(t) = \alpha(0)e^{-i\omega_0 t}$	N/A (see ladder operators)
Ladder Operators	N/A	Annihilation: $\hat{a} = \dfrac{1}{\sqrt{2\hbar Z}}(\hat{\Phi} + iZ\hat{Q})$Heisenberg picture: $\hat{a}(t) = \hat{a}(0)e^{-i\omega_0 t}$
Field Operators	$\Phi(t) = \sqrt{\dfrac{\hbar Z}{2}}(\alpha^*(t) + \alpha(t))$ $Q(t) = i\sqrt{\dfrac{\hbar}{2Z}}(\alpha^*(t) - \alpha(t))$	$\hat{\Phi} = \Phi_{ZPF}(a^\dagger + a)$ $Q = iQ_{ZPF}(a^\dagger - a)$
Impedance Relation	$Z = \sqrt{L/C}$ is the characteristic impedance $\{\Phi, Q\} = 1$ (Poisson bracket)	$Z = \sqrt{L/C}$ $[\hat{\Phi}, \hat{Q}] = i\hbar\hat{\mathbb{1}}$

For the quantum field operators, we used two constants Φ_{ZPF} and Q_{ZPF} that we will define shortly when discussing the eigenvectors of $\hat{H}$.

For typical parameters ($C = 10$ pF, $L = 100$ pH), the resonance frequency is $\omega_0/2\pi \approx 5$ GHz. To observe quantum behavior, we must operate at temperatures where thermal energy is much smaller than the quanta energy ($k_B T \ll \hbar\omega_0$), which requires dilution refrigerators operating at $T \leq 20$ mK. In practice, they operate at 15mK ($-273.13°$C) using dilution refrigerator, see fig. 5 taken from Oxford instrument website.
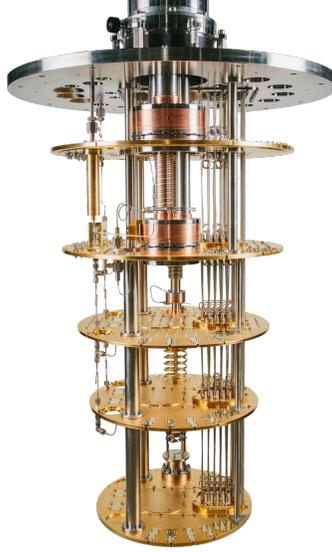
Figure 5: Dilution refrigerator Golden chandeler.

2.3.2 Mechanical ↔ LC Oscillator Correspondence

Before we analyze the Hamiltonian and its eigenvalues, let's pause to compare our quantized LC circuit with the mechanical spring system introduced earlier in the lecture. Drawing on this analogy helps build intuition for how the LC circuit oscillates.

Quantity	Mechanical (spring)	Electrical (LC)
Coordinate	Position $\hat{x}$	Flux Φ
Conjugate Momentum	$\hat{p}$	Charge Q
Mass	m	Capacitance C
Restoring Force	Spring constant k	Inverse Inductance $1/L$
Commutator	$[\hat{x}, \hat{p}] = i\hbar$	$[\hat{\Phi}, \hat{Q}] = i\hbar$

2.4 Fock States of the Quantum Harmonic Oscillator (QHO)

Fock states are the energy eigenstates of the quantum harmonic oscillator (QHO) Hamiltonian and represent distinct, quantized energy levels. The Hamiltonian can be written in terms of ladder operators as

$$\hat{H} = \frac{\hbar\omega_0}{2}(\hat{a}^\dagger\hat{a} + \hat{a}\hat{a}^\dagger) = \cdots = \hbar\omega_0(\hat{a}^\dagger\hat{a} + 1/2)$$

When this Hamiltonian acts on a Fock state $|n\rangle$, the resulting energy eigenvalue E_n is given by

$$\hat{H}|n\rangle = E_n|n\rangle = \hbar\omega_0(n + 1/2)$$

Remember that $\hat{n} = \hat{a}^\dagger\hat{a}$ denotes the number of excitations, and n can take integer values $0, 1, 2, \ldots$ Even in the absence of excitations ($n = 0$), the system possesses energy equal to $1/2\hbar\omega_0$, known as the zero-point energy. This relates to the two constants Φ_{ZPF} and Q_{ZPF} introduced earlier via the statistical mean and variances. **Statistical Mean Values**: Due to the symmetry of Fock states, both the mean flux (Φ) and the mean charge (Q) vanish. For flux, the expectation value is

$$\langle\Phi\rangle_n = \langle n|\Phi_{ZPF}(\hat{a} + \hat{a}^\dagger)|n\rangle = 0$$

9

Similarly, for charge, we have

$$\langle Q \rangle_n = \langle n| -iQ_{ZPF}(\hat{a} - \hat{a}^\dagger)|n\rangle = 0$$

Variance and Zero Point Fluctuations (ZPF): Although the mean values are zero, the fluctuations, measured by the variance, are nonzero and increase with the excitation number n. For example, the variance of flux is given by

$$\mathrm{Var}(\hat{\Phi}) = \langle\hat{\Phi}^2\rangle - \langle\hat{\Phi}\rangle^2 = \cdots = (2n+1)\Phi_{ZPF}^2$$

In the ground state ($n = 0$), the root mean square (RMS) fluctuation, also called the zero point fluctuation, is defined as
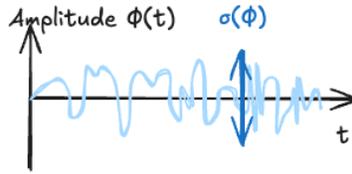
$$\sigma_\Phi(|0\rangle) = \Phi_{ZPF}$$

Figure 6: Zero Point Fluctuation in the phase.

Exercise 7: Zero-Point Fluctuations

Derive the expression $\Phi_{ZPF} = \sqrt{\frac{\hbar Z}{2}}$ starting from $\hat{\Phi} = \Phi_{ZPF}(\hat{a}^\dagger + \hat{a})$ and the variance of the ground state.

Answer

For the ground state $|0\rangle$: $\langle\hat{\Phi}\rangle = 0$ and $\mathrm{Var}(\hat{\Phi}) = \langle\hat{\Phi}^2\rangle$.

$$\hat{\Phi}^2 = \Phi_{ZPF}^2(\hat{a}^\dagger + \hat{a})^2 = \Phi_{ZPF}^2(\hat{a}^{\dagger 2} + \hat{a}^\dagger\hat{a} + \hat{a}\hat{a}^\dagger + \hat{a}^2)$$

Taking expectation in $|0\rangle$: $\langle 0|\hat{a}^{\dagger 2}|0\rangle = 0$, $\langle 0|\hat{a}^2|0\rangle = 0$, $\langle 0|\hat{a}^\dagger\hat{a}|0\rangle = 0$, $\langle 0|\hat{a}\hat{a}^\dagger|0\rangle = 1$.

$$\langle\hat{\Phi}^2\rangle_0 = \Phi_{ZPF}^2$$

The Hamiltonian $\mathcal{H} = \frac{\Phi^2}{2L} + \frac{Q^2}{2C}$ has ground state energy $E_0 = \frac{1}{2}\hbar\omega_0$. By equipartition: $\langle\frac{\Phi^2}{2L}\rangle_0 = \frac{1}{4}\hbar\omega_0 \Rightarrow \Phi_{ZPF}^2 = \frac{\hbar\omega_0 L}{2} = \frac{\hbar}{2}\sqrt{\frac{L}{C}} = \frac{\hbar Z}{2}$

$$\Phi_{ZPF} = \sqrt{\frac{\hbar Z}{2}}$$

We have seen that the system's total energy is divided between the inductive and capacitive forms. The inductive energy is given by

$$E_{ind}(\Phi) = \frac{\Phi^2}{2L}$$

The capacitive energy is

$$E_{cap} = \frac{Q^2}{2C}$$

The variance $\langle \Phi^2 \rangle$ physically represents the extent, or spread, of the wavefunction within the potential well defined by the inductive energy.

As we've discussed, Fock states provide a quantized description of energy in the oscillator, with their wavefunctions displaying characteristic spreads in flux and charge due to zero-point fluctuations. However, to visualize and compare how these quantum states occupy phase space relative to their classical analogs, it is helpful to introduce alternate representations. Particularly, we'll use quasi-probability distributions like the Husimi Q-function. In the following section, we will explore how both classical and quantum states are represented in phase space and better understand the transition from deterministic orbits to the inherently probabilistic nature of quantum mechanics.

2.5   Phase Space Representations: Classical vs. Quantum

In classical mechanics, the state of an oscillator with fixed energy traces a precise elliptical trajectory in the (Φ, Q) phase space. In quantum mechanics, the **Heisenberg**[3] **uncertainty principle** prohibits the simultaneous precise definition of Φ and Q. As a result, a quantum state is described not as a point but as a "cloud" of probability.

The Husimi Q-function provides a useful tool for visualizing this quasi-probability distribution. It is defined by the expression

$$Q(\alpha) = \frac{1}{\pi} \langle \alpha | \rho | \alpha \rangle$$

and represents the expectation value of the density matrix projected onto a coherent state $|\alpha\rangle$. For the ground state $|0\rangle$, the Q-function appears as a Gaussian-shaped blob centered at the origin. Fock states $|n\rangle$ are represented by rings of finite width. In these symmetric states, the quasi-probability density averages to zero at the center. Unlike classical rings, which are depicted as sharp lines, quantum rings exhibit a finite width determined by the Zero Point Fluctuations (Q_{ZPF} and Φ_{ZPF}), see fig. 7.
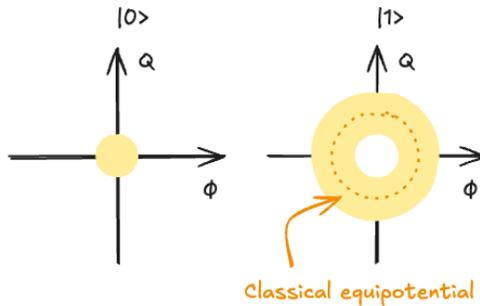

Figure 7: Husimi Q representation of the lowest two energy states.

3   The Transmon Qubit

We begin this section by recalling some important dates of this field of research that started more than 40 years ago. Indeed, the demonstration of the quantized energy levels of a Josephson junction was first achieved in 1985 [4] by John Martinis, Michel Devoret, and John Clarke[4]. That same year marked the creation of

---

[3]Nobel prize in 1932 for the creation of quantum mechanics

[4]Clarke, Devoret and Martinis obtained Nobel prize in 2025 for experiments demonstrating macroscopic quantum mechanical tunnelling and energy quantisation in an electric circuit

the quantronics group at CEA Saclay by Michel Devoret, Daniel Esteve, and Cristian Urbina. Significant progress continued with the development of the Cooper[5] Pair Box in 1999 [5]. This evolution ultimately led to the invention of the Transmon qubit in 2007 [6].
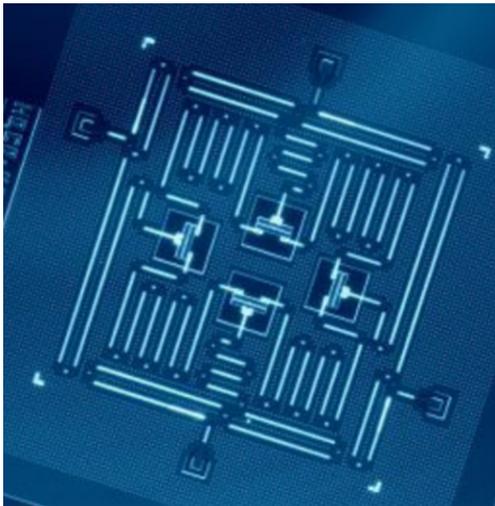

Figure 8: A device consisting of four transmon qubits, four quantum buses, and four readout resonators fabricated by IBM and published in npj Quantum Information in January 2017.

3.1 Why We Need Nonlinearity

A simple LC oscillator is not a qubit, a two-level system. Its energy levels $E_n = \hbar\omega_0(n+1/2)$ are **equidistant**. If we try to drive a transition from $|0\rangle$ to $|1\rangle$ with a microwave pulse at frequency ω_0, we will inadvertently drive transitions to $|2\rangle, |3\rangle$, and so on. We cannot isolate a two-level subspace.

Intuition: The Ladder Problem

Imagine a ladder where every rung is spaced exactly 1 meter apart (harmonic oscillator). To climb it, you use a robot with fixed arms that can only reach exactly 1 meter.

If the robot tries to climb to the first rung, it succeeds perfectly. But because the next rung is also exactly 1 meter away, the robot will keep climbing to the second, third, or fourth rung when you only wanted it to stay on the first one.

To make a qubit, we need to "distort" the ladder. If we make the first rung 1 meter high, but the second rung only 0.9 meters away from the first, the robot can reach the first rung but will fail to reach the second. This unique spacing (anharmonicity) allows us to isolate just the bottom two levels ($|0\rangle$ and $|1\rangle$) and ignore the rest. The Josephson Junction is the component that provides this distortion.

To fix this, we need a non-linear circuit element that makes the energy spacing unequal (anharmonic). This element is the **Josephson Junction**, see fig. 9 extracted from [1].

3.2 Josephson Tunnel Junction

The Josephson Junction (JJ) acts as a **non-linear inductor**, see fig. 10. The energy stored in the junction is given by $\mathcal{E}_J(\phi_j) = E_J \left(1 - \cos\left(\frac{\phi_j}{\Phi_0}\right)\right)$, where $\Phi_0 = \hbar/2e$ is the reduced magnetic flux quantum (approximately 10^{-15} Webers) and ϕ_j is the phase across the junction. By Taylor expanding the cosine term, we can separate the energy into linear and non-linear components:

---

[5]Nobel prize in 1972 for his jointly developed theory of superconductivity, usually called the BCS-theory
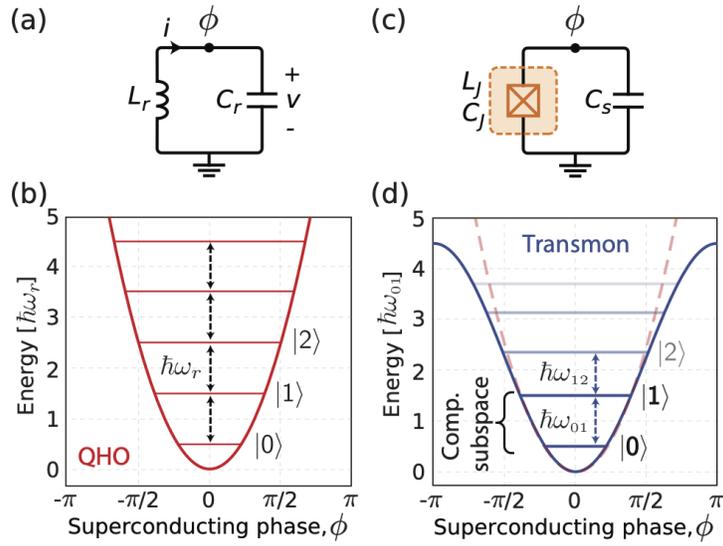
Figure 9: **a** Circuit for a parallel LC-oscillator quantum harmonic oscillator, with inductance L in parallel with capacitance, C. The superconducting phase on the island is denoted ϕ, referencing ground as zero. **b** Energy potential for the QHO, here energy levels are equidistantly spaced $\hbar\omega_r$ apart. **c** Josephson qubit circuit, where the nonlinear inductance L_J, represented with the Josephson-subcircuit in the dashed orange box, is shunted by a capacitance, C_s. **d** The Josephson inductance reshapes the quadratic energy potential, dashed red, into sinusoidal, solid blue, which yields non-equidistant energy levels. This allows us to isolate the two lowest energy levels, forming a computational subspace with an energy separation $\hbar\omega_{01}$, which is different than $\hbar\omega_{12}$.
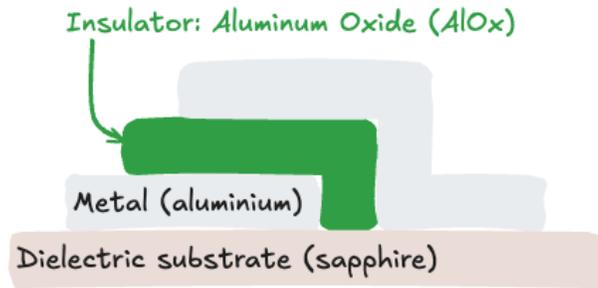

Figure 10: **Schematic cross-section of a Josephson tunnel junction**. Dielectric substrate (light brown): A base layer of Sapphire. Metal (grey): Aluminum electrodes forming the superconducting base and top layers. Insulator (green): A tunnel barrier made of Aluminum Oxide (AlOx) sandwiched between the aluminum layers.

$$\mathcal{E}_J(\Phi_j) = \mathcal{E}_{JJ}^{lin}(\Phi_j) + \mathcal{E}_{JJ}^{NL}(\Phi_j)$$

$$\mathcal{E}_J(\Phi_j) \approx \underbrace{\frac{E_J}{2}\left(\frac{\Phi_j}{\phi_0}\right)^2}_{\text{Linear Inductor}} - \underbrace{\frac{E_J}{4!}\left(\frac{\Phi_j}{\phi_0}\right)^4}_{\text{Non-Linearity}} + \mathcal{O}\left(\Phi_j^6\right)$$

Exercise 8: Taylor Expansion of Cosine

Expand $\cos(x)$ to 4th order and identify the linear and non-linear terms in the Josephson energy.

Answer

Taylor expansion: $\cos(x) = 1 - \frac{x^2}{2!} + \frac{x^4}{4!} - \mathcal{O}(x^6)$ For the Josephson energy with $x = \Phi/\phi_0$:

$$\mathcal{E}_J = E_J(1 - \cos(\Phi/\phi_0)) = E_J\left(\frac{1}{2}\left(\frac{\Phi}{\phi_0}\right)^2 - \frac{1}{24}\left(\frac{\Phi}{\phi_0}\right)^4 + \dots\right)$$

- **Linear term:** $\frac{E_J}{2}\left(\frac{\Phi}{\phi_0}\right)^2 = \frac{\Phi^2}{2L_J}$ with $L_J = \phi_0^2/E_J$ (harmonic inductor) - **Non-linear term:** $-\frac{E_J}{24}\left(\frac{\Phi}{\phi_0}\right)^4$ (provides anharmonicity for qubit)

$\phi_0 = \hbar/2e = 3.3 \times 10^{-16}$ Wb (Weber, unit of magnetic flux) is the magnetic flux quantum with $\hbar$ for the quantum of action, the quantization of energy and the electromagnetic charge of a single electron. The 2 is because we talk about superconductivity so we are interested in pairs of electrons. The **linear term** corresponds to a standard inductor, while the **non-linear term** provides the anharmonicity necessary for qubit operation, to isolate the $|0\rangle \leftrightarrow |1\rangle$ transition.

3.3 Transmon Hamiltonian

A transmon consists of a Josephson Junction in parallel with a large shunting capacitor C, see fig. 9. The large capacitance reduces sensitivity to charge noise, making the qubit stable. The full Hamiltonian is composed of two terms: the junction energy that we just saw ($E_J(\Phi) = -E_J\cos(\Phi/\phi_0)$, where $E_J = \frac{\phi_0^2}{L_J}$) and a capacitive energy, the same as for the QHO ($E_{cap}(\dot{\Phi}) = \frac{1}{2}C\dot{\Phi}^2$). The potential energy thus follows a cosine curve. For small oscillations near the bottom of the well, it behaves like a harmonic oscillator with energy $E_J^{(2)} = \frac{\phi^2}{2L_J}$.

Intuition: The Heavy Shunting Capacitor

The key innovation of the Transmon is the large capacitor in parallel. In our mechanical analogy, this is like making the mass of the spring very heavy.

Why do this? A heavy mass is hard to disturb. In the quantum world, this makes the qubit much less sensitive to "charge noise", aka random fluctuations in the electric environment. This stability comes at a cost: the anharmonicity (the difference between energy levels) gets smaller, but it's a worthy trade-off for a qubit that lives much longer (T_1 and T_2).

Let's get a semi-classical intuition from the Phase Space Picture. We can describe the system using the Hamiltonian $\mathcal{H}$ with conjugate variables Φ (flux) and Q (charge).

$$\mathcal{H}(\phi, Q) = \frac{Q^2}{2C} - E_J \cos\left(\frac{\Phi}{\phi_0}\right)$$

For a standard harmonic oscillator, the energy levels would be:

$$E = \hbar\omega_r(n + 1/2) = \frac{Q^2}{2C} + \frac{\phi^2}{2L_J}$$

In phase space (Q vs Φ), the trajectories of a harmonic oscillator form an **ellipse**. However, the cosine term in the Transmon Hamiltonian deforms these trajectories as the energy increases, leading to **anharmonicity** (uneven spacing between energy levels), see fig. 11.
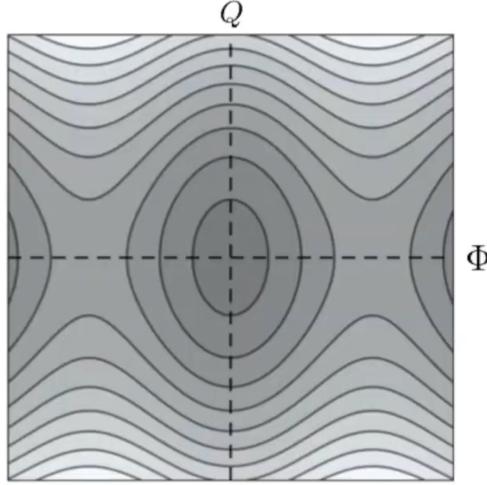

Figure 11: Contour plot of eigenenergies of the phase space (Q vs Φ) of the transmon Hamiltonian.

3.4 Quantum Treatment of the Transmon

Having established the semiclassical and circuit-level understanding of the transmon, we now move to its full quantum description. This section will show how to quantize the transmon Hamiltonian, treat the effects of its nonlinearity, and reveal how the anharmonicity arises, at the origin of the qubit behavior. We start from the Taylor-expanded Hamiltonian:

$$H \simeq \frac{Q^2}{2C} + \frac{\phi^2}{2L_J} - \frac{E_J}{4!}\left(\frac{\Phi}{\phi_0}\right)^4$$

that we rewrite using the creation and annihilation operators $\Phi = \Phi_{ZPF}(a + a^\dagger)$:

$$H = \hbar\omega_0 a^\dagger a - \frac{E_J \phi_{ZPF}^4}{4!}(a + a^\dagger)^4$$

with $\phi_{ZPF} = \Phi_{ZPF}/\phi_0$.

Expanding the $(a + a^\dagger)^4$ term and applying the **Rotating Wave Approximation** to drop fast-oscillating terms (those that do not conserve particle number, e.g., $a^4, (a^\dagger)^4, a^2, (a^\dagger)^2$) we can write the Hamiltonian in the form:

$$\hat{H} = \hat{H}_{stationary} + H_{r(t)}$$

> **Intuition: Rotating Wave Approximation (RWA)**
>
> Imagine pushing a child on a swing. You naturally push at the moment the swing is moving away from you. This effectively adds energy.
> Now imagine you are jittering your hands back and forth really fast while pushing, adding some kind of vibration or shaking. These fast jitters don't really move the swing; they average out to zero over the course of a full swing. The RWA is the mathematical way of saying "ignore the fast jitters that don't match the swing's natural frequency." We keep only the terms that effectively transfer energy.

By expanding the terms, we find that $(a+a^\dagger)^4$ includes terms $\propto a^2, a^\dagger a, (a^\dagger)^2$ and $\propto a^4, a^\dagger a^3, (a^\dagger)^2 a^2, (a^\dagger)^3 a, (a^\dagger)^4$. Terms oscillating at $4\omega_0$, $2\omega_0$, etc., are dropped. We keep only the "stationary" terms and get:

$$H \simeq \hbar\omega_0 a^\dagger a - \frac{E_J}{4!} \cdot \phi_{ZPF}^4 \cdot (12 a^\dagger a + 6 a^{\dagger 2} a^2)$$

> **Exercise 9: Transmon RWA**
>
> Expand $(a + a^\dagger)^4$ and order the terms by their oscillation frequencies.

> **Answer**
>
> $(a + a^\dagger)^4$ gives 16 terms. Grouping by oscillation frequency ($e^{in\omega t}$ in Heisenberg picture):
>
> | Frequency | Terms | Count |
> |---|---|---|
> | $+4\omega$ | $a^{\dagger 4}$ | 1 |
> | $+2\omega$ | $a^{\dagger 3}a, a^{\dagger 2}aa^\dagger, a^\dagger aa^{\dagger 2}, aa^{\dagger 3}$ | 4 |
> | 0 (stationary) | $a^{\dagger 2}a^2, a^\dagger aa^\dagger a, a^\dagger a^2 a^\dagger, aa^\dagger aa^\dagger, a^{\dagger 2}a, a^2 a^{\dagger 2}$ | 6 |
> | -2ω | $a^\dagger a^3, aa^\dagger a^2, a^2 a^\dagger a, a^3 a^\dagger$ | 4 |
> | -4ω | a^4 | 1 |
>
> **RWA keeps only stationary terms** (frequency $= 0$). Using $[a, a^\dagger] = 1$: Stationary terms $\rightarrow 6a^{\dagger 2}a^2 + 12 a^\dagger a + 3$

After grouping terms and accounting for the commutator $[a, a^\dagger] = 1$, we arrive at the standard transmon Hamiltonian:

$$H \simeq \hbar(\omega_0 - \Delta_q)a^\dagger a - \frac{\hbar\alpha}{2} a^{\dagger 2} a^2$$

where:

- $\hbar\Delta_q = \hbar\alpha$ is the Renormalization factor of the linear frequency due to Zero Point Fluctuations (ZPF). This is essentially a **Lamb**[6] **shift** due to ZPF.
- $\hbar\alpha$ is the anharmonicity (also called Kerr nonlinearity), where $\hbar\alpha = \frac{1}{2}E_J\phi_{ZPF}^4$ (zero point fluctuation of the reduced magnetic flux).

We write the hamiltonian in its final form, called a Duffing Oscillator, using the number operator $\hat{n} = a^\dagger a$:

$$H_{RWA} = \underbrace{\hbar\omega_q \hat{n}}_{\text{linear}} - \underbrace{\frac{\hbar\alpha}{2}\hat{n}(\hat{n} - 1)}_{\text{non-linear}}$$

---

[6]Nobel prize in 1955 for his discoveries concerning the fine structure of the hydrogen spectrum

Exercise 10: Duffing Oscillator

Rearrange the expanded Hamiltonian to the form $\hbar\omega_q \hat{n} - \frac{\hbar\alpha}{2}\hat{n}(\hat{n}-1)$.

Answer

Starting from (after RWA): $H = \hbar\omega_0 a^\dagger a - \frac{E_J\phi_{ZPF}^4}{24}(6a^{\dagger 2}a^2 + 12a^\dagger a)$ With $\hbar\alpha = \frac{E_J\phi_{ZPF}^4}{2}$:

$$H = \hbar\omega_0 \hat{n} - \hbar\alpha\hat{n} - \frac{\hbar\alpha}{2}a^{\dagger 2}a^2$$

Note: $a^{\dagger 2}a^2 = a^\dagger(a^\dagger a)a = a^\dagger(\hat{n})a = \hat{n}(\hat{n}-1)$ (using $a\hat{n} = (\hat{n}+1)a$)

$$H = \hbar(\omega_0 - \alpha)\hat{n} - \frac{\hbar\alpha}{2}\hat{n}(\hat{n}-1)$$

Defining $\omega_q = \omega_0 - \alpha$:

$$H = \hbar\omega_q \hat{n} - \frac{\hbar\alpha}{2}\hat{n}(\hat{n}-1)$$

Where $\omega_q = \omega_0 - \Delta_q$ (the "dressed" frequency of the qubit). The energy levels in the system exhibit characteristic transitions. The transition between the first excited state and the ground state is given by $E_1 - E_0 = \hbar\omega_q$. The next transition, from the second excited state to the first, is $E_2 - E_1 = \hbar(\omega_q - \alpha)$. Typical parameter values for these transitions are $\omega_q \sim 5$ GHz for the qubit frequency and $\alpha \sim 0.3$ GHz for the anharmonicity, such that the ratio α/ω_q is approximately 1/10. To first order perturbation theory, only the energy changes, not the wavefunctions (eigenvectors):

- $E_n^{(1)} = \langle n^{(0)}|H_{NL}|n^{(0)}\rangle$
- $|n^{(1)}\rangle = \sum_{k\neq n} \frac{\langle k^{(0)}|H_{NL}|n^{(0)}\rangle}{E_n^{(0)} - E_k^{(0)}}|k^{(0)}\rangle = 0$ since $\langle i|\hat{n}|j\rangle = \delta_{i,j}$

Let's take a numerical example:

Typical Transmon Numerical Parameters

For a standard transmon qubit setup, the following parameter values are used:

Parameter	Symbol	Typical Value / Formula
Inductance	L_J	14 nH
Capacitance	C_J	65 fF
Bare Frequency	$\omega_0 = \sqrt{1/LC}$	5.3 GHz
Josephson Energy	$E_J = \phi_0^2/L_J$	12 GHz
Charging Energy	$E_c = \frac{e^2}{2C}$	0.3 GHz
Impedance	$Z = \sqrt{L/C}$	$\approx 450\ \Omega$
Anharmonicity	α	0.3 GHz
Qubit Frequency	ω_q	≈ 5 GHz

Exercise 11: Anharmonicity

Calculate the anharmonicity α for a transmon with $E_J = 12$ GHz and $E_C = 0.3$ GHz.

> **Answer**
>
> For a transmon, the anharmonicity is given by: $\alpha \approx E_C$ More precisely, from perturbation theory:
> $\hbar\alpha = \frac{E_J \phi_{ZPF}^4}{2}$ with $\phi_{ZPF}^2 = \sqrt{2E_C/E_J}$ This gives: $\alpha = E_C \left(\frac{2E_C}{E_J}\right)^{1/2} \cdot \frac{1}{2}\sqrt{\frac{E_J}{2E_C}} = E_C$ For $E_C = 0.3$ GHz:
>
> $$\alpha \approx 0.3 \text{ GHz} = 300 \text{ MHz}$$
>
> The ratio $E_J/E_C = 12/0.3 = 40 \gg 1$ confirms we're in the transmon regime.

For the zero-point fluctuations, the ratio $Q_{ZPF}/2e \approx 1.0$ which indicates that approximately one Cooper pair is oscillating in the system, which is in stark contrast to the 10^{12} electrons typically involved in motion within classical circuits. For the flux quantum, we have $\Phi_{ZPF}/\phi_0 \approx 0.5$. When the system is in the $|1\rangle$ state, it involves about two Cooper pairs, which underscores the necessity for cryogenic cooling to maintain proper operation.

Finally, to treat the system as a qubit, we restrict the Hilbert space and the operators to the subspace consisting of $\{|0\rangle, |1\rangle\}$. The number operator can then be mapped from $\hat{n} - \frac{1}{2}\hat{\mathbb{I}}$ to $-\frac{1}{2}\hat{Z}$, which is represented as

$$\frac{1}{2}\begin{pmatrix} -1 & 0 \\ 0 & 1 \end{pmatrix}.$$

Similarly, the lowering operator $\hat{a}$ is mapped to $\hat{\sigma} = \frac{1}{2}(X - iY)$, which takes the form

$$\begin{pmatrix} 0 & 1 \\ 0 & 0 \end{pmatrix}.$$

> **Exercise 12: Pauli Matrix Mapping**
>
> Verify that the matrix representations of $\hat{n}$ and $\hat{a}$ in the $\{|0\rangle, |1\rangle\}$ subspace correspond to the Pauli matrices as described.

> **Answer**
>
> In the $\{|0\rangle, |1\rangle\}$ basis: **Number operator:** $\hat{n}|0\rangle = 0$, $\hat{n}|1\rangle = |1\rangle$
>
> $$\hat{n} = \begin{pmatrix} 0 & 0 \\ 0 & 1 \end{pmatrix} = \frac{1}{2}(\mathbb{I} - Z) = \frac{1}{2}\begin{pmatrix} 0 & 0 \\ 0 & 2 \end{pmatrix}$$
>
> Hence $\hat{n} - \frac{1}{2}\mathbb{I} = -\frac{1}{2}Z$
> **Lowering operator:** $\hat{a}|0\rangle = 0$, $\hat{a}|1\rangle = |0\rangle$
>
> $$\hat{a} = \begin{pmatrix} 0 & 1 \\ 0 & 0 \end{pmatrix} = \frac{1}{2}(X + iY) = \sigma_-$$
>
> **Raising operator:** $\hat{a}^\dagger = \begin{pmatrix} 0 & 0 \\ 1 & 0 \end{pmatrix} = \frac{1}{2}(X - iY) = \sigma_+$

We briefly mention that an entire zoo of superconducting qubits exist, depending on the ratio between the physical parameters, see fig. 12 taken from [7]. We can cite the Cooper pair box, flux qubit, phase qubit, quantronium, transmon, fluxonium, and hybrid qubit.
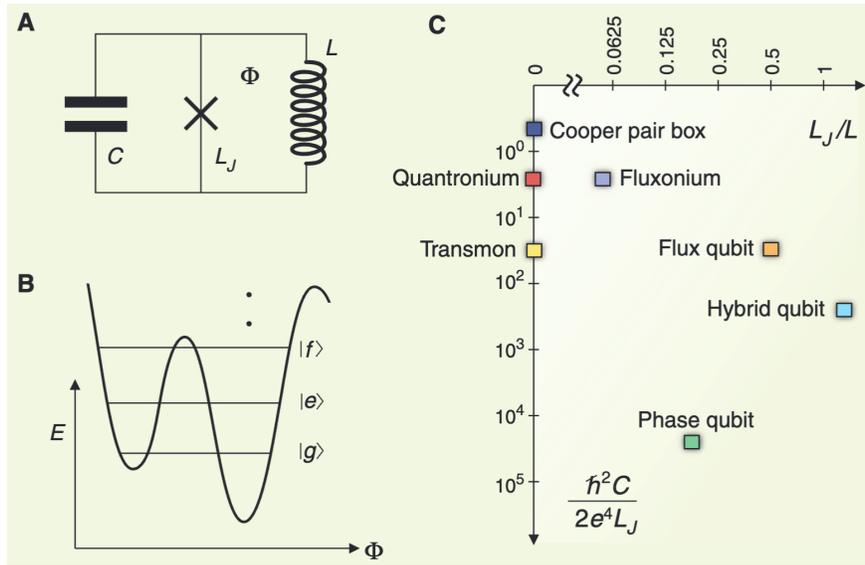
Figure 12: **A** Superconducting qubits consist of simple circuits that can be described as the parallel combination of a Josephson tunnel element (cross) with inductance L_J, a capacitance C, and an inductance L. The flux ϕ threads the loop formed by both inductances. **B** Their quantum energy levels can be sharp and long-lived if the circuit is sufficiently decoupled from its environment. The shape of the potential seen by the flux ϕ and the resulting level structure can be varied by changing the values of the electrical elements. This example shows the fluxonium parameters, with an imposed external flux of $\frac{1}{4}$ flux quantum. Only two of three corrugations are shown fully. **C** A Mendeleev-like but continuous 'table' of artificial atom types: Cooper pair box, flux qubit, phase qubit, quantronium, transmon, fluxonium, and hybrid qubit. The horizontal and vertical coordinates correspond to fabrication parameters that determine the inverse of the number of corrugations in the potential and the number of levels per well, respectively.

3.5 Qubit Control

We end this section by discussing three operations on the isolated transmon qubit: control via 1Q gates, measurement and 2Q gates. To control the qubit, it is coupled to an input/output microwave drive line, typically a coaxial cable, using a capacitor that enables charge-to-charge coupling. The drive Hamiltonian takes the form $H_{drive} = -i\frac{1}{2}\Omega(t)(a^\dagger - a)$, which can be rewritten as $\frac{1}{2}\Omega(t)Y$ for the transmon qubit. The drive signal itself is expressed as $\Omega(t) = \Omega_0 \cdot \sin(\omega_d t + \phi_d)$, where Ω_0 represents the amplitude of the drive and ϕ_d the phase of the drive. We say that the *charge* is coupled since we have $\hat{Q} = -iQ_{ZPF}(a^\dagger - a)$, then the drive Hamiltonian can be interpreted as the drive amplitude multiplied by the number of charge quanta, $H_{drive} = $ ampl. drive $\times \hat{Q}$ quanta.

Exercise 13: Drive Hamiltonian

Show that $H_{drive} \propto \hat{Q}$ leads to σ_y control in the qubit subspace.

Answer

The charge operator: $\hat{Q} = -iQ_{ZPF}(\hat{a}^\dagger - \hat{a})$ The drive Hamiltonian: $H_{drive} = -\frac{i}{2}\Omega(t)(\hat{a}^\dagger - \hat{a}) \propto \hat{Q}$ In the qubit subspace, using $\hat{a} = \sigma_-$ and $\hat{a}^\dagger = \sigma_+$:

$$\hat{a}^\dagger - \hat{a} = \sigma_+ - \sigma_- = \frac{1}{2}(X - iY) - \frac{1}{2}(X + iY) = -iY$$

Therefore:

$$H_{drive} = -\frac{i}{2}\Omega(t)(-iY) = -\frac{\Omega(t)}{2}Y$$

The drive couples to σ_y, enabling rotations around the Y-axis on the Bloch sphere.

The drive signal and the qubit state can be expressed in the rotating frame to understand gate operations. By writing $\sin(\omega_d t + \phi_d) = \frac{i}{2}\left(e^{-i(\omega_d t + \phi_d)} - e^{+i(\omega_d t + \phi_d)}\right)$ and $a(t) = a_0 e^{-i\omega_q t}$, in the initial drive formula $H_{drive} = -i\frac{1}{2}\Omega(t)(a^\dagger(t) - a(t))$, we can apply the Rotating Wave Approximation (RWA) to the drive $(\sigma_- \rightarrow \sigma_- e^{-i\omega_d t})$, and obtain the Hamiltonian in the rotating frame:

$$H_R = \frac{\hbar}{2}\Delta \cdot Z + \frac{\hbar}{2}\Omega\left(e^{-i\phi_d}\sigma_- + e^{i\phi_d}\sigma_+\right).$$

Exercise 14: Rotating Frame Transformation

Apply the unitary $U(t) = e^{i\omega_d t\sigma_z/2}$ to the drive Hamiltonian and derive the time-independent form under RWA.

Answer

Lab frame Hamiltonian: $H = \frac{\hbar\omega_q}{2}\sigma_z + \frac{\hbar\Omega}{2}\cos(\omega_d t + \phi_d)\sigma_y$ Transform to rotating frame with $U(t) = e^{i\omega_d t\sigma_z/2}$:

$$H_R = U^\dagger HU - i\hbar U^\dagger \dot{U} = U^\dagger HU - \frac{\hbar\omega_d}{2}\sigma_z$$

The σ_z term becomes: $\frac{\hbar(\omega_q - \omega_d)}{2}\sigma_z = \frac{\hbar\Delta}{2}\sigma_z$ For the drive, $U^\dagger\sigma_\pm U = e^{\mp i\omega_d t}\sigma_\pm$. Writing $\cos(\omega_d t) = \frac{1}{2}(e^{i\omega_d t} + e^{-i\omega_d t})$: - Terms $\propto e^{\pm 2i\omega_d t}$ oscillate fast $\rightarrow$ drop by RWA - Stationary terms survive Result: $H_R = \frac{\hbar\Delta}{2}\sigma_z + \frac{\hbar\Omega}{2}(e^{-i\phi_d}\sigma_- + e^{i\phi_d}\sigma_+)$

In this interaction picture, the Hamiltonian reduces into two pieces: a first piece that depends on the detuning and sets the amplitude of the rotation at $\Delta = \omega_d - \omega_0$ and another term with (σ_-, σ_+) and depends on the phase of the drive (to choose rotation around the X or Y axis). This Hamiltonian allows for **general rotations on the qubit** by changing Δ and Ω, enabling gates like X, Y, Z, H, S, T. An example is Rabi[7] Oscillations: a constant drive amplitude Ω for a specific time results in a population transfer between $|0\rangle$ and $|1\rangle$.

Having only perfect control through coupling would be ideal. However, control, noise, and dissipation are intrinsically linked. According to the Fluctuation-Dissipation Theorem, coupling to intrinsic I/O (input/output) channels leads to specific relaxation and decoherence times: T_1 the energy relaxation time ($|1\rangle \to |0\rangle$) and T_2, the coherence time (phase information loss).

We saw progress in T_1 times nonetheless: while in the late 90s we had $T_1 \sim 1$ ns, experiments made improvements of roughly 5 orders of magnitude over 20 years, see fig. 13 from [8].
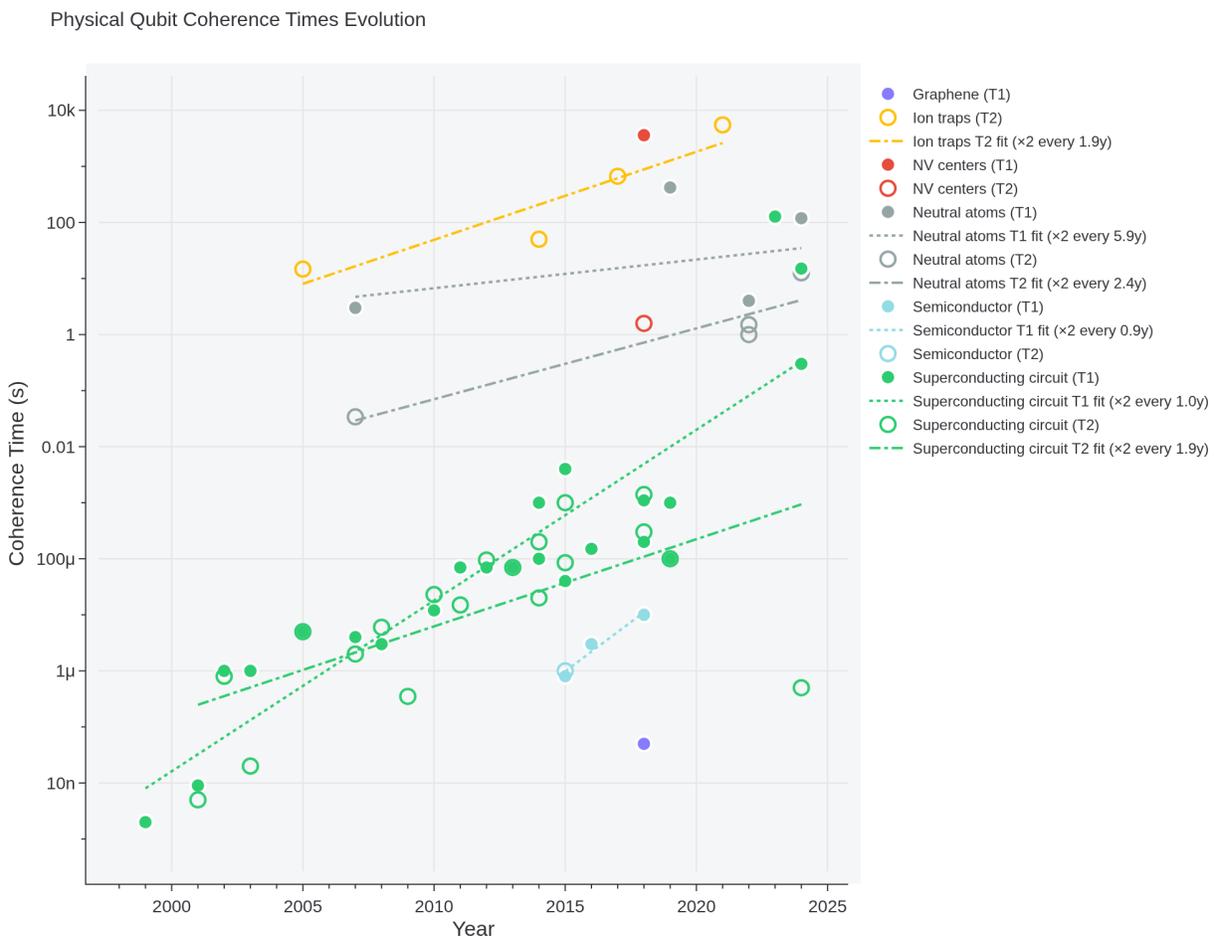

Figure 13: **Physical qubit bitflip and coherence times.** Evolution of reported T_1 in solid lines and T_2 in dashed lines, times across different platforms. An exponential fit showing the characteristic doubling time in years is included. For superconducting circuit, the $T_1 \times 2$ every 0.99y, and for T_2 every 1.94y.

---

[7]Nobel prize in 1944 for his resonance method for recording the magnetic properties of atomic nuclei

3.6 Qubit Measurement Strategies

To measure the qubit, we could couple directly to an I/O transmission line. This approach has the advantage of a simple setup. However, it suffers from the "Purcell" effect (spontaneous emission), which limits T_1 and T_2 because the qubit is too strongly coupled ("open") to its environment. Instead, the qubit is coupled to a detuned microwave cavity (resonator) which is then coupled to the I/O line. In the **dispersive regime** (where the qubit and resonator are detuned), the interaction Hamiltonian is:

$$H_{cav}^{eff} = \hbar \left(\omega_c - \chi\sigma_z\right) a^\dagger a$$

This means the resonator's frequency shifts by $\pm\chi$ depending on whether the qubit is in $|0\rangle$ or $|1\rangle$. By measuring the reflection of a probe signal off the resonator, we can infer the qubit state without destroying it.

Intuition: The Refractive Index Analogy

How do we measure the qubit without touching it? Imagine the qubit is a piece of glass inside the cavity. When the qubit is in state $|0\rangle$, the glass has one refractive index. When it's in state $|1\rangle$, the index changes slightly.

This change shifts the resonant frequency of the cavity. By sending a tone into the cavity and seeing if it reflects or transmits, we can determine the "color" (frequency) of the cavity and thus deduce the state of the qubit. This is "dispersive" because it relies on the dispersion (frequency shift) rather than absorption of energy.

Exercise 15: Dispersive Shift

Using second-order perturbation theory on the Jaynes-Cummings Hamiltonian, derive the dispersive shift $\chi = g^2/\Delta$.

Answer

Jaynes-Cummings Hamiltonian: $H = \hbar\omega_c a^\dagger a + \frac{\hbar\omega_q}{2}\sigma_z + \hbar g(a^\dagger\sigma_- + a\sigma_+)$ In the dispersive regime $|\Delta| = |\omega_q - \omega_c| \gg g$, treat coupling as perturbation. Unperturbed states: $|n,g\rangle$, $|n,e\rangle$ with energies $E_{n,g} = n\hbar\omega_c - \frac{\hbar\omega_q}{2}$, $E_{n,e} = n\hbar\omega_c + \frac{\hbar\omega_q}{2}$
Second-order energy shift for $|n,g\rangle$:

$$E_{n,g}^{(2)} = \frac{|\langle n-1, e|H_{int}|n,g\rangle|^2}{E_{n,g} - E_{n-1,e}} = \frac{\hbar^2 g^2 n}{-\hbar\Delta} = -\frac{\hbar g^2 n}{\Delta}$$

Similarly for $|n,e\rangle$: $E_{n,e}^{(2)} = +\frac{\hbar g^2 (n+1)}{\Delta}$
Effective Hamiltonian: $H_{eff} = \hbar(\omega_c + \chi\sigma_z)a^\dagger a$ with $\chi = g^2/\Delta$

This **Quantum Non-Demolition (QND)** setup inhibits spontaneous emission. The measurement mechanism relies on the fact that the reflection of the I/O line at the resonator depends on the qubit's state. Oscillators are used for both readout and facilitating **2-qubit (2Q) gates**.

3.7 Two Coupled Transmon Qubits

We saw how to perform single qubit gates on the transmon and how to measure its state. The last piece is how to generate entanglement between tramson qubits. When two transmons (or a transmon and a resonator) are coupled via a capacitor, the system is described by individual Hamiltonians:

- **Qubit 1:** $H_1 = \frac{Q_1^2}{2C_a} - E_a \cos\left(\frac{\phi_1}{\Phi_0}\right)$
- **Qubit 2:** $H_2 = \frac{Q_2^2}{2C_b} - E_b \cos\left(\frac{\phi_2}{\Phi_0}\right)$

The total Hamiltonian can be separated into linear and non-linear parts ($H_{full} = H_{lin} + H_{NL}$): The linear part corresponds to the Hamiltonian of the two QHO which is $H_{lin} = \hbar\omega_a a^\dagger a + \hbar\omega_b b^\dagger b$. The non-Linear Part is Derived from the Taylor expansion of the cosine potential for both transmons:

$$\mathcal{E}_J(\phi) = -E_J \cos\left(\frac{\Phi}{\phi_0}\right) \simeq \frac{E_J}{2!}\left(\frac{\Phi}{\phi_0}\right)^2 - \frac{E_J}{4!}\left(\frac{\Phi}{\phi_0}\right)^4 + \mathcal{O}(\Phi^6)$$

$$H_{NL} = -\frac{E_a}{4!}\left(\frac{\Phi_1}{\phi_0}\right)^4 - \frac{E_b}{4!}\left(\frac{\Phi_2}{\phi_0}\right)^4$$

Because they are coupled, the physical fluxes ϕ_1, ϕ_2 are functions of the normal mode operators a and b: $\phi_1 = f(\phi_a, \phi_b)$ and $\phi_2 = g(\phi_a, \phi_b)$. In their quantized form, we look for fluxes as: $\phi_1 = \phi_{1a}^{ZPF}(a^\dagger + a) + \phi_{1b}^{ZPF}(b^\dagger + b)$.

Notice that we could apply this method in the case of readout, where one system is the **cavity** (resonator) and the other is the **qubit**. We have the following linear terms:

$$H_{lin} = \underbrace{\hbar\omega_c a_c^\dagger a_c}_{\text{cavity}} + \underbrace{\hbar\omega_q a_q^\dagger a_q}_{\text{qubit}}.$$

The non-linear coupling is expressed as:

$$H_{NL} = -\frac{E_a}{4!}\left(\phi_{1a}^{ZPF}(a^\dagger + a) + \phi_{1b}^{ZPF}(b^\dagger + b)\right)^4$$

From which we derive the standard dispersive regime interaction Hamiltonian. One important limitation is that this approach is inherently limited to nearest-neighbor coupling. Indeed, the two qubits must be connected via a physical electrical circuit, a capacitor in our example. This implies that multiple $SWAP$ gates are necessary, which will limit the length of quantum computation possible before decoherence.

4 Bosonic Encoding

4.1 Bosonic Modes and Open Systems

4.1.1 Why Bosonic Modes?

After discussing how a two-level transmon can be encoded in a QHO, we revisit the QHO and its "ladder" of energy states. Previously, we chose to encode our two-level system using the lowest two energy levels, which necessitated introducing anharmonicity so that these states could be manipulated independently without inadvertently affecting higher levels. However, encoding information in a QHO is not limited to just its ground and first excited states. Instead, any two specific states among the infinite set of resonator states can be selected, including states constructed as clever superpositions. We denote these specially chosen states as $|0_L\rangle$ and $|1_L\rangle$, using the subscript L to indicate their role as logical qubit states within the QHO. For instance, we could have chosen specific Fock state combination like $|0\rangle_L = \frac{1}{\sqrt{2}}(|0\rangle + |4\rangle)$ and $|1\rangle_L = |2\rangle$, this is the Kitten code, more on this code below. This approach to encoding information in QHO or bosonic modes is known as a bosonic code. Bosonic modes provide several practical advantages. First, they offer hardware efficiency because information can be encoded in high-dimensional Hilbert spaces. Second, high-Q resonators serving as bosonic modes can exhibit much longer coherence times than traditional qubits, resulting in longer lifetimes for the encoded information. Third, established techniques for microwave state manipulation enable robust control of these bosonic modes. Finally, the errors encountered in such systems are typically simpler, with photon loss being the predominant type of error.

Moving from the ideal QHO to open systems requires us to account for environmental interactions such as photon loss and dephasing. Our first step is to write down the equation of motion that describes these open systems, introduce an nice visualization tool, and examine different examples of QHO behavior.

4.1.2 The Lindblad Master Equation

First, to describe the evolution of a state in a QHO, the "simple" Schrödinger[8] equation is not enough. We have to include environmental interactions. The evolution of the density matrix ρ is described by the more complicated equation, the master equation:

$$\dot{\rho} = -i[H, \rho] + \sum_k \mathcal{D}_{L_k}\rho.$$

Where the Lindbladian dissipator is given by $\mathcal{D}_L\rho = L\rho L^\dagger - \frac{1}{2}\{L^\dagger L, \rho\}$, which governs the non-unitary evolution induced by dissipation. Here, the curly brackets $\{\cdot, \cdot\}$ denote the anticommutator, defined for operators A and B as $\{A, B\} = AB + BA$. In this context, H still represents the system Hamiltonian. The new operators L_k correspond to the dissipation, or jump, operators that capture the effects of the environment on the system.

Exercise 16: Lindblad Equation

Verify that the Lindblad equation preserves the trace of the density matrix ($\mathrm{Tr}(\dot{\rho}) = 0$).

Answer

Lindblad equation: $\dot{\rho} = -i[H, \rho] + \sum_k \mathcal{D}_{L_k}\rho$ with $\mathcal{D}_L\rho = L\rho L^\dagger - \frac{1}{2}\{L^\dagger L, \rho\}$
Hamiltonian term: $\mathrm{Tr}(-i[H, \rho]) = -i\mathrm{Tr}(H\rho - \rho H) = -i(\mathrm{Tr}(H\rho) - \mathrm{Tr}(H\rho)) = 0$
Dissipator term:

$$\mathrm{Tr}(\mathcal{D}_L\rho) = \mathrm{Tr}(L\rho L^\dagger) - \frac{1}{2}\mathrm{Tr}(L^\dagger L\rho) - \frac{1}{2}\mathrm{Tr}(\rho L^\dagger L)$$

Using cyclic property: $\mathrm{Tr}(L\rho L^\dagger) = \mathrm{Tr}(L^\dagger L\rho)$

$$= \mathrm{Tr}(L^\dagger L\rho) - \frac{1}{2}\mathrm{Tr}(L^\dagger L\rho) - \frac{1}{2}\mathrm{Tr}(L^\dagger L\rho) = 0$$

Therefore $\mathrm{Tr}(\dot{\rho}) = 0$, preserving $\mathrm{Tr}(\rho) = 1$.

4.1.3 Coherent States

Before introducing the visualizing tool for quantum states of a QHO in phase space, it is essential to introduce the class of **coherent states**, which are the "most classical" states of the quantum harmonic oscillator. A coherent state $|\alpha\rangle$ is defined as the eigenstate of the annihilation operator $\hat{a}$:

$$\hat{a}|\alpha\rangle = \alpha|\alpha\rangle$$

where α is a complex number.

Mathematically, in the Fock state basis, a coherent state is expressed as a superposition of number states weighted by Poissonian amplitudes:

$$|\alpha\rangle = e^{-|\alpha|^2/2} \sum_{n=0}^{\infty} \frac{\alpha^n}{\sqrt{n!}}|n\rangle$$

The probability to find n photons in a coherent state follows a Poisson distribution, given by $P(n) = |\langle n|\alpha\rangle|^2 = e^{-|\alpha|^2}\frac{|\alpha|^{2n}}{n!}$.

---

[8]Nobel prize in 1933 for the discovery of new productive forms of atomic theory

Exercise 17: Coherent State Poissonian

Show that the probability distribution $P(n) = |\langle n | \alpha \rangle|^2$ for a coherent state is Poissonian with mean $\bar{n} = |\alpha|^2$.

Answer

Coherent state: $|\alpha\rangle = e^{-|\alpha|^2/2} \sum_{n=0}^{\infty} \frac{\alpha^n}{\sqrt{n!}} |n\rangle$

Probability: $P(n) = |\langle n | \alpha \rangle|^2 = e^{-|\alpha|^2} \frac{|\alpha|^{2n}}{n!}$

This is precisely the Poisson distribution with parameter $\lambda = |\alpha|^2$.

Mean: $\bar{n} = \langle \alpha | \hat{n} | \alpha \rangle = \langle \alpha | a^\dagger a | \alpha \rangle = |\alpha|^2$ (since $a|\alpha\rangle = \alpha|\alpha\rangle$)

Variance: $\mathrm{Var}(n) = \langle n^2 \rangle - \langle n \rangle^2 = |\alpha|^2 = \bar{n}$

Equal mean and variance confirms Poissonian statistics.

Physically, a coherent state can be created by displacing the vacuum state $|0\rangle$ in phase space. The displacement operator is defined as:

$$D(\alpha) = e^{\alpha \hat{a}^\dagger - \alpha^* \hat{a}}$$

Thus, $|\alpha\rangle = D(\alpha)|0\rangle$.

Intuition: Coherent States

A coherent state $|\alpha\rangle$ is the quantum state that most closely resembles a classical oscillating field. Imagine a pendulum swinging with a large amplitude. In the quantum world, the trajectory of the "tip" of the pendulum isn't a point in phase space, but a small fuzzy ball of uncertainty (the zero-point fluctuation).

In a coherent state, this fuzzy ball swings back and forth without spreading out or changing shape. It stays "coherent." The distance from the center tells you the number of photons (energy), while the angle tells you the phase of the oscillation.

Exercise 18: Displaced Vacuum is a Coherent State

Prove that applying the displacement operator $D(\alpha)$ to the vacuum state $|0\rangle$ yields the coherent state $|\alpha\rangle$ defined as the eigenstate of the annihilation operator: $a|\alpha\rangle = \alpha|\alpha\rangle$.

Hints:
- Consider the Baker-Campbell-Hausdorff (BCH) formula for operator exponentials.
- Write $|\alpha\rangle = D(\alpha)|0\rangle$ and act with a on this state.
- Show explicitly that $aD(\alpha)|0\rangle = \alpha D(\alpha)|0\rangle$.

Answer

Define $|\alpha\rangle \equiv D(\alpha)|0\rangle$ with $D(\alpha) = e^{\alpha a^\dagger - \alpha^* a}$.

Key identity: $D^\dagger(\alpha) a D(\alpha) = a + \alpha$ (displacement transforms a)

Proof of identity: Using BCH, $e^{-A} B e^A = B + [B, A] + \frac{1}{2!}[[B, A], A] + \dots$ With $A = \alpha a^\dagger - \alpha^* a$ and $B = a$: $[a, \alpha a^\dagger] = \alpha$, higher commutators vanish.

Show eigenvalue equation:

$$a|\alpha\rangle = aD(\alpha)|0\rangle = D(\alpha) \underbrace{D^\dagger(\alpha) a D(\alpha)}_{=a+\alpha} |0\rangle$$

$$= D(\alpha)(a + \alpha)|0\rangle = D(\alpha)(0 + \alpha|0\rangle) = \alpha D(\alpha)|0\rangle = \alpha|\alpha\rangle$$

One idea that will become important in the next section is to focus on the parity of such states. Understanding the parity of coherent states gives us physical intuition for phase space representations like the Wigner function. The parity operator is defined as $\hat{\Pi} = (-1)^{\hat{n}}$. The average parity of a quantum state is the difference between the probability of having an even number of photons and an odd number of photons:

$$\langle \Pi \rangle = P(\text{even}) - P(\text{odd}) = \sum_{n=0}^{\infty} (-1)^n P(n)$$

For the vacuum state $|0\rangle$ (which is a coherent state with $\alpha = 0$), the distribution is $P(0) = 1$ and all other $P(n) = 0$, so the parity is exactly $+1$. But what is the parity of a coherent state far from the vacuum state? For a coherent state with large energy (large $|\alpha|$), the photon number distribution $P(n)$ becomes a wide bell curve centered at $\bar{n} = |\alpha|^2$. Because this distribution is smooth and spreads across many integers, the probability of having n photons (even) is almost exactly the same as having $n + 1$ photons (odd). Therefore, the positive and negative terms in the parity sum cancel each other out:

$$\langle \Pi \rangle_\alpha = \underbrace{P(0) - P(1)}_{\approx 0} + \underbrace{P(2) - P(3)}_{\approx 0} + \cdots \approx 0$$

Mathematically, the expectation value of parity for a coherent state is $\langle \alpha | \hat{\Pi} | \alpha \rangle = e^{-2|\alpha|^2}$. For example, if $\alpha = 3$, this value is $e^{-18} \approx 10^{-8}$, confirming the intuitive "perfect cancellation." This will explain why the Wigner function (understood as a parity expectation) of the vacuum state $|0\rangle$ is zero far from the origin, this is the topic of the next section.

4.1.4 The Wigner Function Definition and Intuition

In the previous sections, we referred to phase space several times to visualize the possible trajectories of the system. Now, to fully characterize quantum states of a QHO in phase space, a nice tool is the Wigner[9] function, a powerful tool for visualizing state evolution. The Wigner function $W(x, p)$ is a quasi-probability distribution that represents a quantum density matrix $\hat{\rho}$ in phase space. In the context of a Quantum Harmonic Oscillator (QHO), regions where the Wigner function takes on negative values directly indicate the presence of quantum behavior.

> **Intuition: The Topography of Quantum States**
>
> Think of the Wigner function as a topographic map of the quantum state in phase space.
> - **Hills (Positive):** Where the particle is likely to be found (like a probability distribution).
> - **Valleys (Negative):** This is where it gets weird. Negative probabilities don't exist in the classical world. A negative value in the Wigner function is a smoking gun for quantum interference effects. It's the signature that says "this is definitely not just a classical noisy system."

Mathematically, the Wigner function is defined as

$$W(x, p) = \frac{1}{\pi \hbar} \int_{-\infty}^{+\infty} \langle x + y | \hat{\rho} | x - y \rangle e^{-2ipy/\hbar} dy$$

---

[9]Nobel prize in 1963 for his contributions to the theory of the atomic nucleus and the elementary particles

Exercise 19: Wigner Function Norm

Show that the integral of the Wigner function over all phase space is normalized to unity: $\int W(x, p)dxdp = 1$.

Answer

Using the definition: $W(x, p) = \frac{1}{\pi\hbar} \int_{-\infty}^{+\infty} \langle x + y|\rho|x - y\rangle e^{-2ipy/\hbar}dy$

Integrate over p: $\int_{-\infty}^{+\infty} e^{-2ipy/\hbar}dp = 2\pi\hbar \cdot \delta(2y) = \pi\hbar \cdot \delta(y)$

Thus: $\int W(x, p)dp = \frac{1}{\pi\hbar} \int \langle x + y|\rho|x - y\rangle \cdot \pi\hbar\delta(y)dy = \langle x|\rho|x\rangle$

Now integrate over x:

$$\int\int W(x, p)dxdp = \int \langle x|\rho|x\rangle dx = \text{Tr}(\rho) = 1$$

The Wigner function is a proper quasi-probability distribution (integrates to 1).

From this expression alone it can be hard to grasp the physics of it. From an intuitive perspective, the value of the Wigner function at a given complex point α in phase space is proportional to the expectation value of a displaced parity operator:

$$W(\alpha) \propto \langle\psi|D(\alpha)\hat{\Pi}D^\dagger(\alpha)|\psi\rangle$$

Here, the parity operator is given by $\hat{\Pi} = (-1)^{a^\dagger a}$ (the parity of excitations), which can also be written as $e^{-i\pi a^\dagger a}$. The displacement operator is $D(\alpha) = e^{\alpha a^\dagger - \alpha^* a}$. For instance, the operator transformation $D^\dagger(\alpha)aD(\alpha) = a + \alpha$ demonstrates how displacement acts on the annihilation operator. Similarly, applying the displacement operator to the vacuum state as $D(\alpha)|0\rangle = |\alpha\rangle$ produces a coherent state. We will use Wigner representations of states a lot in this last section, starting with some simple examples of dissipation.

Displacement Operator vs. Lindblad Dissipator

The displacement operator $D(\alpha)$ (which shifts states in phase space) should not be confused with the Lindblad dissipator $\mathcal{D}_L(\rho)$ (which describes environmental dissipation). In these notes, D always denotes the displacement operator for phase space translations, not a dissipative process.

4.1.5 Examples of Dissipation

To illustrate Wigner representation from Lindblad master equations and to introduce the cat qubit as our first example of bosonic code, we first look at cavities with photon loss.

4.1.5.1 Simple Photon Loss Photon loss or loss of excitation from the cavity to the environment is the predominant type of error in QHO. When the dissipation operator is $L = \sqrt{\kappa_1}a$, the evolution of the system is described by the equation

$$\dot{\rho} = \kappa_1 \left(a\rho a^\dagger - \frac{1}{2}a^\dagger a\rho - \frac{1}{2}\rho a^\dagger a\right)$$

As time progresses, the system settles into the vacuum state independently of the initial state, which means $\lim_{t\to\infty} \rho(t) = |0\rangle\langle 0|$. In the phase space representation, such as a Wigner function, the state can be seen spiraling toward the origin.

4.1.5.2   Locality in Phase Space of the Damped Cavity   An important point that motivates the study of bosonic modes is the locality of errors in phase space, such as photon loss. The Wigner representation indeed reveals that for QHO, errors occurring at high rates are usually the result of local processes within phase space. Mathematically, this behavior is captured by the Fokker-Planck[10] Equation.

In the case of a damped cavity characterized by a loss rate κ_1, the master equation $\dot{\rho} = \kappa_1 \mathcal{D}_a \rho$ can be translated into its phase space evolution as

$$\frac{d}{dt} W_\rho(\alpha, \alpha^*) = \underbrace{\frac{\kappa_1}{2} \frac{\partial^2}{\partial \alpha \partial \alpha^*} W_\rho(\alpha, \alpha^*)}_{\text{Diffusion (broadening)}} + \underbrace{\frac{\kappa_1}{2} \left(\frac{\partial}{\partial \alpha} \alpha + \frac{\partial}{\partial \alpha^*} \alpha^* \right) W_\rho(\alpha, \alpha^*)}_{\text{Global drift towards vacuum}}$$

The diffusion term leads to a broadening of the distribution over time. At the same time, global drift acts to pull the state back toward the vacuum state $|0\rangle$, which corresponds to the origin of phase space. Encoding information in the Hilbert space of the QHO is a form of non-local encoding well suited to fight local errors, just like quantum error correction, as we will see in the next lectures.

4.1.5.3   Driven Damped Cavity   Let's look at another example of QHO dynamics, this time a bit more complex. When the system has both a drive Hamiltonian, given by $H = \varepsilon_1 a^\dagger + \varepsilon_1^* a$, and the same loss term as in the previous example $L = \sqrt{\kappa_1} a$, the master equation can be recast using a shifted operator $a - \alpha$ as follows:

$$\dot{\rho} = \mathcal{D}_{\sqrt{\kappa_1}(a-\alpha)} \rho$$

Here, the displacement α satisfies $\alpha = -\frac{2i\varepsilon_1}{\kappa_1}$, which is equivalent to $\frac{\kappa_1 \alpha}{2} = -i\varepsilon_1$.

To see this, consider the outlined mathematical derivation. First, we expand the driven master equation:

$$\dot{\rho} = -i[\varepsilon_1 a^\dagger + \varepsilon_1^* a, \rho] + \kappa_1 \left(a\rho a^\dagger - \frac{1}{2} a^\dagger a \rho - \frac{1}{2} \rho a^\dagger a \right)$$

By carrying out algebraic manipulations, this master equation can be simplified and rewritten in terms of the dissipator for a displaced operator:

$$\dot{\rho} = \mathcal{D}_{\sqrt{\kappa_1} a} \rho + \left[\frac{\kappa_1 \alpha}{2} a^\dagger, \rho \right]$$

This driven-damped system stabilizes to a coherent state $|\alpha\rangle$ as defined in the previous section. >

4.2   Cat Code: Two-Photon Driven Damped QHO

Encoding information is not possible in a single photon driven damped oscillator, because the kernel of its effective dissipation consists of only a single state. To enable information encoding, we require the kernel of the dissipative dynamics to have higher dimension. We can achieve this by squaring the terms in the Lindblad master equation, which intuitively results in a two-dimensional kernel. Such a configuration gives rise to the formation of **Schrödinger Cat states**.

The Hamiltonian for this system is given by $H = \varepsilon_2 a^{\dagger 2} + h.c.$ The dissipation operator takes the form $L = \sqrt{\kappa_2} a^2$. The equation of motion is expressed as $\dot{\rho} = \mathcal{D}_{\sqrt{\kappa_2}(a^2 - \alpha^2)} \rho$. At steady state, the displacement is $\alpha = \pm \sqrt{\frac{-2i\varepsilon_2}{\kappa_2}}$. In phase space, the system stabilizes into two distinct lobes in the x-p plane, which correspond to a superposition of two coherent states.

Physically, these systems are realized by coupling multiple resonators to induce nonlinear interactions through 4-wave mixing. The experimental setup includes two coupled oscillators, denoted as modes $\hat{a}$ and $\hat{d}$, which are connected to a drive line by means of a coupling capacitor. The drive Hamiltonian is $H_d = \varepsilon_d d^\dagger$ and the interaction between the modes is mediated by 4-wave mixing. The effective Hamiltonian describing this

---

[10]Max Planck received the Nobel prize in 1918 for the discovery of energy quanta

interaction is $H = g_2 a^{\dagger 2} d + g_2 a^2 d^{\dagger}$. For simplicity, this can be modeled with the operators mentioned above: $H_{eff} = \varepsilon_2 a^{\dagger 2} + h.c.$ and the effective dissipation operator $L_{eff} = \sqrt{\kappa_2} a^2$.

In this system, two coherent states, $|\alpha\rangle$ and $|-\alpha\rangle$, are stabilized and can be identified with the logical qubit states. The logical $|0\rangle_L$ state corresponds to $|\alpha\rangle$, while the logical $|1\rangle_L$ state corresponds to $|-\alpha\rangle$.

Intuition: Schrödinger Cat States

Why "Cat"? In Schrödinger's thought experiment, the cat is in a superposition of "Dead" and "Alive." These are two macroscopic, distinguishable states.

Here, our "Dead" and "Alive" states are $|\alpha\rangle$ (oscillation with phase 0) and $|-\alpha\rangle$ (oscillation with phase π) respectively. These are macroscopically distinct states of the field. A "Cat State" is a quantum superposition of these two ($|\alpha\rangle + |-\alpha\rangle$). In phase space, you see two distinct blobs (the cat is definitely either dead or alive if you look classically) but with interference fringes between them (the quantum proof that it's both at once).

The even cat state, $|+\rangle$, is proportional to $|\alpha\rangle + |-\alpha\rangle$ and can be written as

$$|+\rangle \propto |\alpha\rangle + |-\alpha\rangle \propto \sum_n \frac{\alpha^{2n}}{\sqrt{(2n)!}} |2n\rangle$$

The odd cat state, $|-\rangle$, is proportional to $|\alpha\rangle - |-\alpha\rangle$ and is given by

$$|-\rangle \propto |\alpha\rangle - |-\alpha\rangle \propto \sum_n \frac{\alpha^{2n+1}}{\sqrt{(2n+1)!}} |2n+1\rangle$$

Exercise 20: Cat State Parity

Show that $|+\rangle \propto |\alpha\rangle + |-\alpha\rangle$ contains only even photon numbers by expanding the coherent states in the Fock basis.

Answer

Expand coherent states: $|\alpha\rangle = e^{-|\alpha|^2/2} \sum_{n=0}^{\infty} \frac{\alpha^n}{\sqrt{n!}} |n\rangle$

For $|-\alpha\rangle$: $|-\alpha\rangle = e^{-|\alpha|^2/2} \sum_{n=0}^{\infty} \frac{(-\alpha)^n}{\sqrt{n!}} |n\rangle = e^{-|\alpha|^2/2} \sum_{n=0}^{\infty} \frac{(-1)^n \alpha^n}{\sqrt{n!}} |n\rangle$

Sum: $|\alpha\rangle + |-\alpha\rangle = e^{-|\alpha|^2/2} \sum_{n=0}^{\infty} \frac{\alpha^n (1 + (-1)^n)}{\sqrt{n!}} |n\rangle$

Note that $1 + (-1)^n = \begin{cases} 2 & \text{if } n \text{ even} \\ 0 & \text{if } n \text{ odd} \end{cases}$

Therefore: $|+\rangle \propto |\alpha\rangle + |-\alpha\rangle = 2e^{-|\alpha|^2/2} \sum_{k=0}^{\infty} \frac{\alpha^{2k}}{\sqrt{(2k)!}} |2k\rangle$

Only even Fock states $|0\rangle, |2\rangle, |4\rangle, \ldots$ contribute $\rightarrow$ **even parity**

These logical states represent a qubit with its associated Bloch sphere illustrated in figure fig. 14.
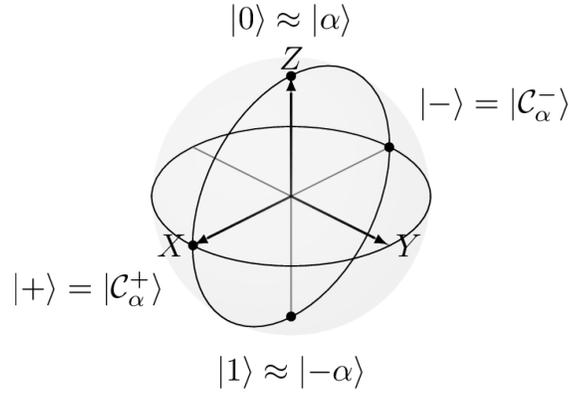
Figure 14: Bloch sphere representation of the cat qubit, as a two-level system encoded in the infinite-dimensional Hilbert space of a harmonic oscillator.

Logical State	Notation	Phase Space Representation
Zero	$\lvert 0 \rangle_L \approx \lvert \alpha \rangle$	
One	$\lvert 1 \rangle_L \approx \lvert -\alpha \rangle$	
Plus	$\lvert + \rangle_L \propto \lvert \alpha \rangle + \lvert -\alpha \rangle$	
Minus	$\lvert - \rangle_L \propto \lvert \alpha \rangle - \lvert -\alpha \rangle$	

A key objective is to suppress bit-flip (X) errors. Using coherent states that are well separated in phase space causes their overlap, which produces errors, to become exponentially small. The overlap between two coherent states $\lvert \alpha \rangle$ and $\lvert -\alpha \rangle$ is $\langle \alpha \lvert -\alpha \rangle = e^{-2\lvert \alpha \rvert^2}$ As $\lvert \alpha \rvert^2$ increases, this overlap and therefore the probability of local error processes decreases exponentially. Hence, the bit-flip time T_X grows exponentially as $\lvert \alpha \rvert^2$ increases, see fig. 15 from [9]. In contrast, the phase-flip rate Γ_Z increases linearly with α^2, see fig. 16 from [9]. Indeed, increasing $\lvert \alpha \rvert^2$ also results in smaller interference fringes in phase space, making the system more susceptible to phase-flip (Z) errors. The ratio between phase-flip and bit-flip error probabilities has reached values of up to

$$\frac{P_Z}{P_X} = 10^7 \quad \text{at } \lvert \alpha \rvert^2 = 10$$

> **Exercise 21: Coherent State Overlap**
>
> Calculate the overlap $\lvert \langle \alpha \lvert -\alpha \rangle \rvert^2$ and confirm that it decays exponentially with $\lvert \alpha \rvert^2$.
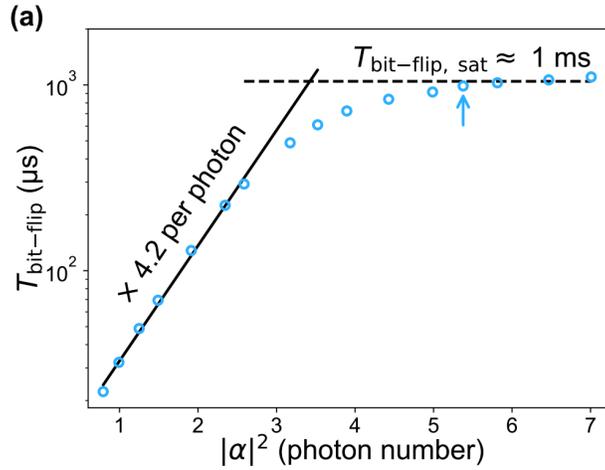
(a)

Figure 15: Exponential increase of the bit-flip time with the cat size.
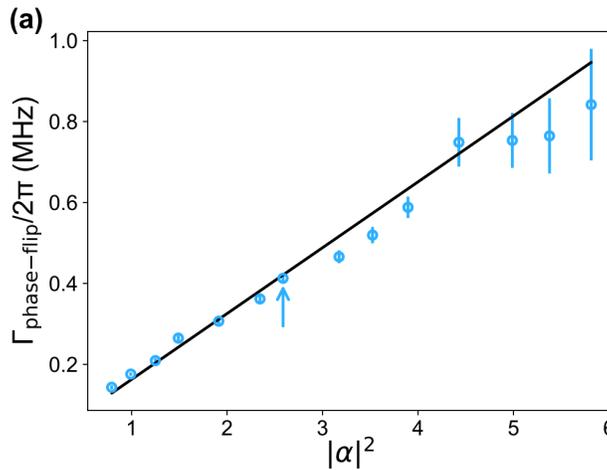
(a)

Figure 16: Linear increase of the phase-flip rate with the cat size.

One possible strategy for a Fully Protected Qubit involves considering simpler quantum error correction code, specifically 1D instead of 2D codes. This topic will be discussed in detail in the QEC lecture. Other bosonic qubits exist, but we are not going to discuss them in this lecture. We only mention that Cat code belongs to a broader family of Rotationally Symmetric Codes (rotational symmetry referring to the Wigner representation). This family includes the 4-Component Cat Code, where four coherent states are used to

encode the logical information ($|0\rangle_L \propto |\alpha\rangle + |i\alpha\rangle + |-\alpha\rangle + |-i\alpha\rangle$), allowing for better error detection of photon loss. Another code robust against single photon loss is the much simpler Kitten code defined with $|0\rangle_L = \frac{1}{\sqrt{2}}(|0\rangle + |4\rangle)$ and $|1\rangle_L = |2\rangle$, where a photon loss event changes the parity of the logical states. Finally, we have to mention a translationally symmetric code known as the GKP (from Gottesman, Kitaev and Preskill) code. This code encodes a qubit in grid states of light and is robust against small displacements in phase space. We end this section by focusing on operations that preserve the noise bias of cat qubits, called bias preserving operations.

4.3 Bias Preserving Operations

Having described how bosonic modes are encoded, we now discuss the process of performing operations on them, focusing in particular on the cat code. When working with qubits that have biased noise, it is essential that operations do not convert the suppressed error type into a more dominant one.

A standard Hadamard gate is thus not suitable in this context because it swaps X and Z errors, thereby destroying the noise bias. Instead, only certain operations are permissible: $Z(\theta)$ rotations, Pauli X, CNOT (CX) gates, and Toffoli ($CCNOT$ or CCX) gates.

The parity state preparation $\mathcal{P}_{|+\rangle}$ is implemented by starting from the state $|0\rangle$, conserving parity throughout the operation, and finally arriving at the state $|+\rangle$. A $Z(\theta)$ rotation is described by the master equation

$$\dot{\rho} = -i\varepsilon_Z[a + a^\dagger, \rho] + \kappa_2 \mathcal{D}_{a^2 - \alpha^2}\rho$$

where ε_Z is a real parameter. To effectively maintain protection of the code space, it is required that κ_2 is much greater than ε_Z. To implement a logical X gate while still preserving the noise bias, the quantum state is rotated within phase space. The evolution of the system during this operation follows the equation

$$\dot{\rho} = -i[-\frac{\pi}{T}\hat{a}^\dagger\hat{a}, \rho] + \mathcal{D}_{\hat{q} - \alpha(t)}\rho$$

in which $\alpha(t) = \alpha e^{i\pi t/T}$. The mechanism relies on physically rotating the state in the complex plane over a period T. During this rotation, strong dissipation as described by the $\mathcal{D}$ term provides error protection by keeping the state pinned to the appropriate moving coherent states and thus suppressing bit-flip errors.

The CNOT gate is realized as a conditional operation that depends on the state of the control qubit, labeled as qubit 1. In operator form, the CNOT can be expressed as

$$CNOT = \frac{1}{2}(\mathbb{I}_1 + Z_1)\mathbb{I}_2 + \frac{1}{2}(\mathbb{I}_1 - Z_1)X_2.$$

An equivalent projection representation is

$$\approx |\alpha\rangle\langle\alpha| \otimes \mathbb{I}_2 + |-\alpha\rangle\langle-\alpha| \otimes X_2.$$

This means that if the control qubit is in the $|\alpha\rangle$ state, the target qubit remains unchanged, while if the control is in the $|-\alpha\rangle$ state, an X gate is applied to the target. The evolution of the system during the CNOT gate is governed by the equation

$$\dot{\rho} = -i[\hat{H}, \rho] + \kappa_2 \mathcal{D}_{\hat{a}_1^2 - \alpha_1^2}\rho + \kappa_2 \mathcal{D}_{\hat{a}_2^2 - \frac{1}{2}\alpha(\hat{a}_1 + \alpha) + \frac{1}{2}\alpha e^{\frac{2i\pi t}{T}}(\hat{a}_1 - \alpha)}\rho.$$

where $\hat{H} = \frac{1\pi}{2T}\frac{\hat{a}_1 - \alpha}{2\alpha} \otimes \left(\hat{a}_2^\dagger\hat{a}_2 - \bar{n}\right) + \text{h.c.}$ to compensate for non-adiabatic errors, just like for the X gate.

References

1. Krantz, P. *et al.* A Quantum Engineer's Guide to Superconducting Qubits. *Applied Physics Reviews* **6**, 021318 (2019).
2. Joshi, A., Noh, K. & Gao, Y. Y. Quantum information processing with bosonic qubits in circuit QED. *Quantum Science and Technology* **6**, 033001 (2021).

3. Dirac, P. A. M. & Dirac, P. A. M. *The Principles of Quantum Mechanics.* (Oxford University Press, Oxford, New York, 1981).

4. Martinis, J. M., Devoret, M. H. & Clarke, J. Energy-Level Quantization in the Zero-Voltage State of a Current-Biased Josephson Junction. *Phys. Rev. Lett.* **55**, 1543–1546 (1985).

5. Nakamura, Y., Pashkin, Y. A. & Tsai, J. S. Coherent control of macroscopic quantum states in a single-Cooper-pair box. *Nature* **398**, 786–788 (1999).

6. Koch, J. *et al.* Charge-insensitive qubit design derived from the Cooper pair box. *Physical Review A* **76**, (2007).

7. Devoret, M. H. & Schoelkopf, R. J. Superconducting Circuits for Quantum Information: An Outlook. *Science* **339**, 1169–1174 (2013).

8. Le Régent, F.-M. Awesome Quantum Computing Experiments: Benchmarking Experimental Progress Towards Fault-Tolerant Quantum Computation. (2025) doi:10.48550/arXiv.2507.03678.

9. Lescanne, R. *et al.* Exponential suppression of bit-flips in a qubit encoded in an oscillator. *Nature Physics* **16**, 509–513 (2020).